



**NTNU – Trondheim**  
Norwegian University of  
Science and Technology

# CFD modeling for direct liquefaction of biomass in hydrothermal media

**Alizeb Hussain Syed**

Master's Thesis

Submission date: August 2013

Supervisor: Khanh-Quang Tran, EPT

Co-supervisor: Ilkka Turunen, Lappeenranta University of Technology

Norwegian University of Science and Technology  
Department of Energy and Process Engineering



**MASTER THESIS**

for

Stud.techn. Alizeb Hussain Syed

Spring 2013

*CFD modeling for direct liquefaction of biomass in hydrothermal media*

**Background and objective**

Hydrothermal processing is a promising technology for converting plant biomass directly to liquid fuels with better fuel properties. The technology employs water, in sub or supercritical conditions as reaction media, and therefore is very suitable for wet biomass feedstock including agricultural waste. It can also be employed as pre-treatment of plant biomass for bio-ethanol production and biomass combustion. However, some aspects of the technology are not fully understood and still disputed. More research in this area is needed, particularly for Norwegian plant biomass, to have better understandings and insights into the technology.

This project will theoretically assess the use of hydrothermal media for direct liquefaction of biomass in a continuous flow tubular reactor using Ansys Fluent.

**The following tasks are to be considered:**

1. Literature study on CFD modeling for hydrothermal liquefaction of biomass in continuous flow tubular reactors .
2. Selection and construction a physical model for the reactor
3. CFD modeling for the reactor with non-reacting fluid flow containing particles.
4. CFD modeling for the reactor with reacting fluid flow containing no particles.
5. CFD modeling for the reactor with reacting fluid flow containing biomass particles.
6. Validation of the predicted results
7. Writing technical reports and a master thesis

-- “ --

Within 14 days of receiving the written text on the master thesis, the candidate shall submit a research plan for his project to the department.

When the thesis is evaluated, emphasis is put on processing of the results, and that they are presented in tabular and/or graphic form in a clear manner, and that they are analyzed carefully.

The thesis should be formulated as a research report with summary both in English and Norwegian, conclusion, literature references, table of contents etc. During the preparation of the text, the candidate should make an effort to produce a well-structured and easily readable report. In order to

ease the evaluation of the thesis, it is important that the cross-references are correct. In the making of the report, strong emphasis should be placed on both a thorough discussion of the results and an orderly presentation.

The candidate is requested to initiate and keep close contact with his/her academic supervisor(s) throughout the working period. The candidate must follow the rules and regulations of NTNU as well as passive directions given by the Department of Energy and Process Engineering.


Risk assessment of the candidate's work shall be carried out according to the department's procedures. The risk assessment must be documented and included as part of the final report. Events related to the candidate's work adversely affecting the health, safety or security, must be documented and included as part of the final report. If the documentation on risk assessment represents a large number of pages, the full version is to be submitted electronically to the supervisor and an excerpt is included in the report.

Pursuant to "Regulations concerning the supplementary provisions to the technology study program/Master of Science" at NTNU §20, the Department reserves the permission to utilize all the results and data for teaching and research purposes as well as in future publications.

The final report is to be submitted digitally in DAIM. An executive summary of the thesis including title, student's name, supervisor's name, year, department name, and NTNU's logo and name, shall be submitted to the department as a separate pdf file. Based on an agreement with the supervisor, the final report and other material and documents may be given to the supervisor in digital format.


- Work to be done in lab (Water power lab, Fluids engineering lab, Thermal engineering lab)  
 Field work

Department of Energy and Process Engineering, 11. March 2013



---

Olav Bolland  
Department Head



---

Quang Tran  
Academic Supervisor

**Thesis title: CFD Modeling for Direct Liquefaction of Biomass in Hydrothermal Media**

**Summary:**

The first generation biofuels which is coming from food crops for instance grain and sugar beet are inadequate to achieve desirable oil products because of the scarcity to food supply, therefore the importance of second generation biofuels has increased. Another advantage of second generation biofuel is that the feedstock (non-food-biomass) could be farmed for energy purposes, which enables better production per unit area of the land; and we could utilize the land efficiency. The feedstock of 2nd generation biofuels which are ligno-cellulose in nature includes cereal straw, bagasse, forest residue and vegetable grasses.

This project has theoretically assessed the use of hydrothermal media for direct liquefaction of biomass in a continuous flow tubular reactor using ANSYS Fluent and other relevant software's. Micro-reactor is considered for better heat and mass transfer, also micro-reactor provides admissible control over unwanted side reactions. The exact reaction path of biomass dissociation is unknown therefore lumped kinetic is considered for model species like cellulose, hemicellulose and lignin.

Computationally the velocity, temperature distribution, reaction kinetic, feed percentage and particle modeling are examined. It is being vindicated by results that the effect of fluid velocity over reactor domain is tremendous, and has high influence on temperature profile inside the reactor. The geometry of different dimensions is also investigated, which play integral role in the system. Furthermore, the effect of large or small eddies is examined by weightless particle and discussed in the result section. The optimum biomass particle size is proposed, which is suitable for our system.

For future work, the predicted operating conditions for micro flow tubular reactor by simulation must be validated by experimental work. This computation work will facilitate and provide essential information to start experimental work.

*Name: Alizeb Hussain, Syed*

*Date: 02.08.2013*

*Supervisor: Associate Professor Khanh-Quang Tran.*

*Co-Supervisor: Professor Ilkka Turunen*

# ACKNOWLEDGEMENTS

---

I would like to say thanks to Almighty ALLAH (GOD) for his blessing and mercy.

This thesis will not be accomplished without the kind suggestions, discussions and comments of Associate Professor Khanh-Quang Tran. I have no words to say thanks to him for being so helpful throughout this research. I also want to say thanks to Professor Ilkka Turunen for his guidance and concern.

I would like to say thanks to staff members of NTNU and LUT, especially to Minna Loikkanen for her prompt help while I was away from Finland. Lastly I would like to gratitude my family for their support and pray.

I dedicate this thesis research to my Mother and my elder brother.



# Table of Contents

---

1	Introduction.....	1
1.1	General .....	1
1.2	Objectives .....	3
1.3	Tasks of the Thesis Research .....	3
2	Background.....	5
2.1	Biomass .....	5
2.1.1	Cellulose .....	6
2.1.2	Hemi-Cellulose .....	6
2.1.3	Lignin.....	7
2.2	Micro-Reactor .....	8
2.3	Super-Subcritical Water and Its Importance in Liquefaction Process. ....	9
2.4	Biomass Conversion Techniques for Energy Applications .....	12
2.4.1	Hydrothermal Liquefaction Process (HTL) .....	14
2.5	Kinetic Model.....	15
2.5.1	Kinetic Model of Cellulose.....	16
2.5.2	Kinetic Model of Lignin .....	17
2.5.3	Kinetic Model of Hemi-cellulose.....	19
2.6	Turbulence Model .....	20
2.7	Reynolds Number of the Flow .....	21
2.8	Turbulence Intensity (T.I) .....	21
2.9	Multiphase Model.....	22



2.9.1	Continuity Equation of Mixture Model .....	22
2.9.2	Momentum Equation of Mixture Model.....	23
2.9.3	Energy Equation of Mixture Model.....	23
2.9.4	Relative (slip) Velocity and Drift velocity.....	23
3	Method of Study .....	24
3.1	General .....	24
3.2	Selection and Construction a Physical Model.....	25
3.3	Modeling for Reactor Containing Particles.....	25
3.4	Modeling of Reaction.....	26
3.5	Modeling of Real Biomass Particles .....	27
4	Results and Discussions.....	28
4.1	Selection and Construction a Physical Model.....	28
4.1.1	Geometry Construction.....	28
4.1.2	Effect of Velocity on Outlet Temperature .....	30
4.1.3	Effect of Velocity on Actual System .....	34
4.1.4	Velocity Effect on Double Inlet for Super/Subcritical water.....	35
4.1.5	Effect of Inlet Diameter .....	37
4.2	Modeling for Reactor Containing Particles.....	38
4.2.1	Biomass Feed Effect .....	38
4.2.2	Particle Movement inside the Reactor .....	40
4.3	Modeling of Reactions .....	42
4.3.1	Density of Sub/Supercritical Water inside the Reactor .....	42
4.3.2	Reactions by ANSYS Fluent .....	43
4.3.3	Reactions by MATLAB .....	45

4.3.4	Effect of temperature on cellulose conversion.....	47
4.4	Modeling of Real Biomass Particle.....	48
5	Conclusions.....	51
6	Future Works .....	52
7	Reference .....	53
	Appendix A: Non-Linear Arrhenius Parameter for Hemi-cellulose .....	58
	Appendix B: Geometry of difference dimensions .....	59
	Appendix C: Histogram values .....	60
	Appendix D: Contour of glucose and lignin-product mass fractions .....	61
	Appendix E: MATLAB files .....	62
	Appendix F: Viscosity and Conductivity inside the reactor; calculated by ANSYS fluent .....	65
	Appendix G: Modeling of Particles at different sizes (50,150,600 and 1100) mm.	66

# List of Figures

---

Figure 1 Internal structure of Biomass(Lope Tabil 2011) .....	5
Figure 2 the molecular structure of cellulose and its dissociated form.....	6
Figure 3 Hemi-cellulose structure and its degraded products under the influence of H <sup>+</sup> ions .....	7
Figure 4 Lignin molecular structure .....	8
Figure 5 comparison between micro-reactor and conventional reactor mixing. ....	9
Figure 6 Thermodynamic properties of water as a function of temperature at 25MPa(Pooya Azadia 2011).....	11
Figure 7 the combustion of biomass particles as a function of time.....	12
Figure 8 the thermochemical conversion of biomass(Mustafa Balat 2009) .....	14
Figure 9 phase diagram of water, indicating operating conditions of hydrothermal liquefaction	15
Figure 10 reaction path of lignin at subcritical water .....	18
Figure 11 examined geometry of 1.8mm diameter. ....	28
Figure 12 opted and developed geometry for our system.....	29
Figure 13 the biomass is introduced from upper inlet with 0.4m/s increased velocity, whereas the supercritical water is introduced from left hand side with low velocity of 0.3 m/s.....	30
Figure 14 the biomass is introduced from upper inlet with low velocity of 0.3m/s, whereas the supercritical water is introduced from left hand side with high velocity of 0.4 m/s.....	31
Figure 15 the velocity effect of biomass solution on outlet boundary at constant velocity of supercritical water. ....	31
Figure 16 the velocity effect of supercritical water on outlet boundary at constant velocity of biomass solution.....	32
Figure 17 the biomass solution velocity is 0.1m/s and supercritical water is at 0.3m/s. ....	33
Figure 18 Histogram profile of figure17 outlet surface, y-axis is the percentage of each temperature portion.....	33
Figure 19 the velocity of biomass solution is 0.2m/s whereas the velocity of supercritical water is 0.4m/s.....	34
Figure 20 the velocity of biomass solution is 0.4m/s whereas the velocity of supercritical water is 0.2m/s.....	35
Figure 21 the velocity of biomass solution and supercritical water is 0.3m/s each.....	35

Figure 22 the velocity of biomass solution is 0.01m/s whereas the velocity of supercritical water is 0.2m/s each.....	36
Figure 23 histogram of figure 22 outlet surface, y-axis is the percentage of each temperature portion.....	37
Figure 24 the effect of 3mm double inlet of supercritical water.....	38
Figure 25 temperature distribution inside the reactor with 10% biomass solution by weight.....	39
Figure 26 temperature distribution inside the reactor with 7% biomass solution by weight.....	39
Figure 27 relative velocity of biomass solution and supercritical water along the length of reaction at position (0,3) .....	41
Figure 28 weightless particles is introduced from biomass inlet surface (0,3)position.....	41
Figure 29 Yoshio Masuda introduced weightless particle from right hand side of the mixer.....	42
Figure 30 density of water along the length of reactor at position (0,3).....	43
Figure 31 the non-converge residues(y-axis)of cellulose and lignin until the 7000 iterations.....	44
Figure 32 decomposition of species as a function of time.....	46
Figure 33 decomposition of lignin as a function of time.....	46
Figure 34 conversion of cellulose as a function of temperature.....	47
Figure 35 red dots represent the diameter of particle, which is 10microns in this case.....	49
Figure 36 red dots represent the diameter of particle, which is 100microns in this case.....	49
Figure 37 red dots represent the diameter of particle, which is 500microns in this case.....	50
Figure 38 red dots represent the diameter of particle, which is 1000microns in this case.....	50

# List of Tables

---

Table 1 physical properties of water.....	10
Table 2 conversion of cellulose at subcritical temperature.....	17
Table 3 the quality parameters of geometry and mesh .....	29

# 1 Introduction

## 1.1 General

The first generation biofuels which is coming from food crops like grain and sugar beet are inadequate to achieve desirable oil products because of the scarcity to food supply, therefore the importance of second generation biofuels has increased. Another advantage of second generation biofuel is that the feedstock (non-food-biomass) could be farmed for energy purposes, which enables better production per unit area of the land; and we could utilize the land efficiency. The feedstock of 2nd generation biofuels which are ligno-cellulose in nature includes cereal straw, bagasse, forest residue and vegetable grasses (Taylor 2008, Singhb 2011). It is generally believe that the ligno-cellulose is low in costs due to the high production along with energy and environmental benefits. The Ligno-cellulose is abundantly available in the world with 10-50 billion annual production. The energy produce by biomass is renewable and CO<sub>2</sub> neutral (Kamimoto 2006). The structure of biomass is composed of cellulose 40-50%, hemicellulose 20-25% and 20-25% is lignin(J. Perez 2002).

The commercial investment has been made in Bio-refinery by Royal Nedalco, Logen, Diversa Celunol, Abengoa and DuPont for the production of bioethanol. These plants are using ligno-cellulose as raw material, which is in early stage and need to be developed for 50-150MI/year approximately in near future. The bio-refinery is an expensive process that includes the total fixed capital of around162-200million USD. The commercial production of second generation biofuels is in the developing stage, therefore more research and development is required in bio-refinery for commercial usage. And (Taylor 2008).

To rectify and minimize the cost of production, the hydrothermal liquefaction could play an integral role. Hydrothermal processing is a promising technology for converting plant biomass directly to liquid fuels with better fuel properties than obtained by conventional fast pyrolysis(Zhang, Huang et al. 2012). The technology employs water, in sub or supercritical conditions as reaction media, and therefore is also suitable for wet biomass feedstock like agricultural waste. The subcritical and supercritical water is considered to be favorable for liquefaction process because of low O/C ratio in products and using water as reacting medium(Marrone 2012). At critical temperature, water has tendency to solubilize non-polar

components. The critical water which is solvent and reactant could dissolve biomass of high moisture content directly. The hydrothermal liquefaction process does not require pre-treatment processes like dewatering or drying which are recommended process for other conversion techniques. The end products of this process are not completely soluble in water, which favours cost saving separation process. The energy consumption of HTL process is *about 10-15 percent of the energy in the feedstock biomass, yielding an energy efficiency of 85-90 percent* (Becker 2013, Energy 2013).

The control on temperature facilitates significant to improve the rate of reaction rate and selectivity of the product. In sub and supercritical water it is observed that the yields of desirable products are far away from practical purpose; because of side reaction, which is generated due to prolong high temperature. It is important that substrate (biomass) temperature must be raised fast to critical point for reaction. Therefore, micro-reactor play an essential role for controlling and raising the temperature of biomass quickly to improve product yield (Yoshio Masuda 2006).

The liquefaction process includes hundreds of reactions and products under the presence of critical water. The complete reaction mechanism of biomass conversion is still undiscovered. Many researchers have used lump kinetic to get an idea about possible reaction path and they are successful in it too. For simplification the scientists have used model component of biomass for instance cellulose, hemi-cellulose and lignin. According to Olanrewaju and Zhang that the cellulose under the influence of critical water decomposes into glucose and by-products (Olanrewaju 2012, Zhang, Huang et al. 2012). Furthermore, the glucose continues to decompose into fructose and other by-products (Zhang 2008). In case of lignin, (Matsumura 2012) presented that the lignin decompose into guaiacol, gas, TOC (other liquid products), aromatic hydrocarbon (benzene, naphthalene and toluene), phenol, char, catechol, 0-cresol and m-cresol. However Matsumura mentioned that the dominant products of lignin are TOC, gas and char. The study on hemi-cellulose in subcritical water is very limited and only few numbers of articles are available until now. The hemi-cellulose consists of consecutive reactions initially it decomposes into xylose-oligomers, then xylose and lastly into degraded products. (Mazza 2010).

The application of Computational Fluid Dynamics (CFD) in biomass conversion is tremendous. (B. Potic 2005, Yan 2008, Cai Y Ma 2011) have used CFD for studying heat transfer phenomenon in supercritical water and for thermochemical conversion of biomass. With CFD B.Potic, Yan and Cai have predicted the thermodynamic properties of their system. It is always

advisable to simulate the problem computationally before performing experimental work because it saves time and finance also. Later on the simulated results is validated via experimental work.

## 1.2 Objectives

To study the direct liquefaction of biomass in subcritical water using computational fluid dynamics (CFD). The prime focus is on computational work (ANSYS fluent software) for investigating the behavior of tubular micro flow reactor at elevated temperature. Secondly we examine the reacting flow of the biomass containing particles.

## 1.3 Tasks of the Thesis Research

### 1. Physical model for the reactor

Prolong heating time is a disadvantage because it provokes unwanted side products; therefore spontaneous temperature rise of substrate is a key element. For this purpose, the physical properties of the flow are studied to overcome the side products problems. We have considered following criteria for physical models:

- Uniform distribution of temperature i.e. No/less hot spots inside the system.
- Temperature rise of substrate solution in fraction of second.
- Optimum mixing inside the system.
- Optimum operating conditions for post processing i.e. Micro-reactor.

### 2. Simulation of reactor with biomass containing particles and its feed effect

The developed physical model in task 1 is used to study the model component of biomass. The model components of biomass are cellulose, lignin and hemicellulose. We study the biomass feed percentage and its effect on distribution of temperature. In addition to this, we validate no formation of small or large eddies by mean of weightless particle that causes rotation effects inside the system.

### 3. Reaction kinetic parameters for biomass

Since many researchers have done experimental work and have found reaction kinetic parameters for liquefaction of biomass, therefore in this task we opted/manipulated those parameters into our system. The prime concern is to choose most relevant parameters and reaction path that could be implemented into CFD. The yield of model components will be studied along with the temperature effect on the conversion.



#### **4. Simulation of reacting biomass and the effect of particle diameter**

Using ANSYS fluent software, the particle size of the biomass is studied. The optimum diameter will be investigated inside the reactor. The particles should not block inside the system, also the particles must be kept away from the wall boundaries. Ideally, the particles must be dispersed and apart from each other, so that they are more exposed to critical water for reactions.

## 2 Background

### 2.1 Biomass

The availability of biomass is abundant in most parts of the earth. Biomass is becoming one of the core and most prominent source of renewable energy nowadays, because of acceptable energy density(S and 2011). Based upon conversion techniques the biomass has different end products; in case of liquefaction the end products are mainly bio-gas and water soluble components(Tom Bruton 2009).The general sources of biomass are agricultural, forest, municipal, energy and biological. The agricultural biomass consist of food grain, bagasse known as crushed sugarcane, straw, seed hulls, nutshells, corn stalks, manure of cattle, hogs, and poultry. The forest biomass is classified as woody waste, bark or wood, trees, timber slash, mill scrap and sawdust. The municipal biomass is divided into RDF (refuse derived fuel), paper waste, sewage sludge, yard clippings and food waste. The sources of energy biomass are alfalfa, switch grass, willows, poplars, prairie bluestem, corn, canola, soybean and other plant oils. The biological biomass is mainly animal waste, biological waste and aquatic species (Basu 2010). The main components in biomass are carbon, hydrogen, oxygen and nitrogen; which form different molecular compounds for instance starch, lignin, hemi-cellulose and other hydro-carbon chains. The lignocellulose biomass are the major part of biomass, they are non-starch parts of biomass. Due to non-starch property of lignocellulose, they could easily be used for fuel without threaten the food supply for the world. The lignocellulose is mainly consisted of cellulose, hemi-cellulose and lignin. (Peter Quaak 1999, N.L Panwara 2012).

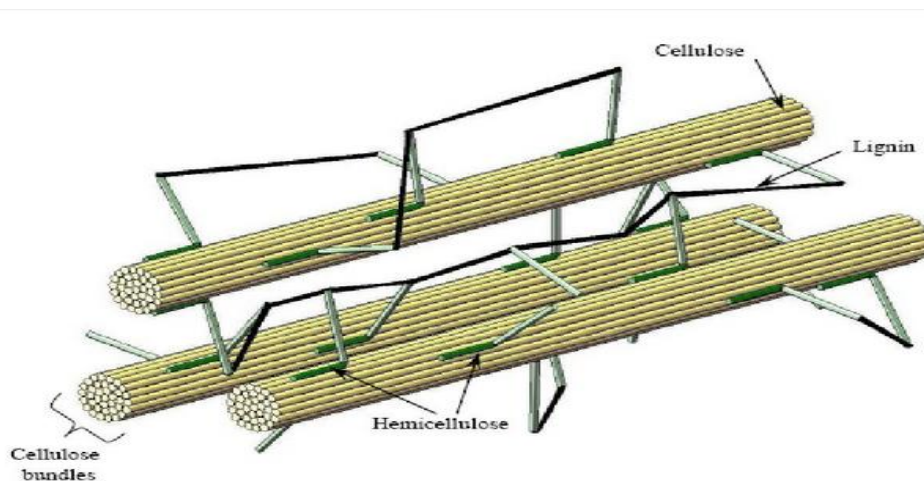


Figure 1 Internal structure of Biomass(Lope Tabil 2011)

### 2.1.1 Cellulose

Cellulose is considered to be an abundant organic component which is available on earth. Cellulose has an average molecular weight range of 300 000–500 000, depending upon the length of the cellulose chain. The average molecular weight of cellulose is measured the degree of polymerization (DP). The molecular structure of cellulose consist of polysaccharide with a glucose monomer unit and  $\beta$ -1,4 glycoside linkages(Valery B. Agbor 2011) . The repeating unit of cellulose polymer constituent of cellobiose, in addition the cellulose could be reflected as a condensation polymer of glucose(Bansal P 2010, Sunky Park 2010). The solubility of cellulose in water is low or sparingly soluble due to its internal structure i.e. dominant crystalline region holds with hydrogen bonds. The crystalline region of cellulose decrease incredibly with pretreatment. The act of acids, alkalis and hydrolysis could rapture the crystalline region and degrades the celluloses(Abhijit Shrotri). The molecular structure and dissociation of cellulose in water is mentioned in figure2:

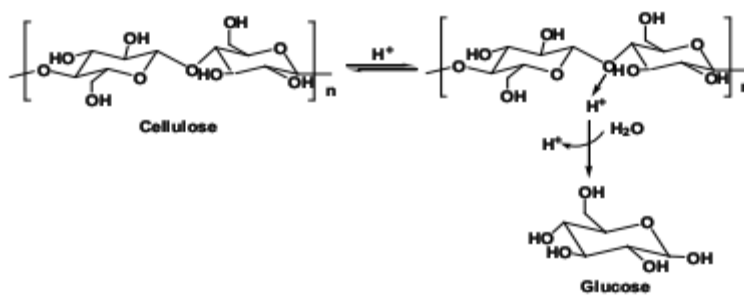


Figure 2 the molecular structure of cellulose and its dissociated form.

### 2.1.2 Hemi-Cellulose

Hemicellulose is a polysaccharide which is consisted of monosaccharide units. It is usually branched with DP ranging from less than 100 to about 200 units. The monosaccharide buildup of sugars 5C's component namely xylose and arabinose, 6C's sugars namely glucose, mannose and galactose. The residues are galacturonic acid and O-methyl-glucuronic acid(Dinesh Mohan 2006). Most often in hemicellulose, the prominent component is xylan which comprises of xylose monomer. Relatively to cellulose, the hemi-cellulose structure is less crystalline and tends to be amorphous because of branched structure. The degradation of hemi-cellulose under the influence of subcritical temperature, chemicals, alkali and acid medium would be easier than

cellulose(Wyman 2000). The molecular structure of hemi-cellulose is showed in figure 3(Bell 2012).

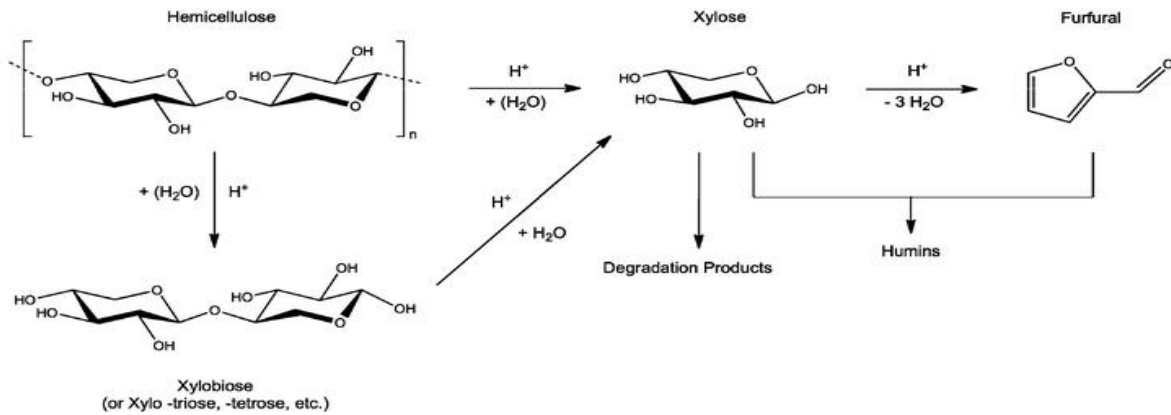


Figure 3 Hemi-cellulose structure and its degraded products under the influence of H<sup>+</sup> ions

### 2.1.3 Lignin

Lignin is connected with cellulose and hemicellulose component to build up lignocellulose compounds. This connection of lignin needs to be ruptured to make lignin reachable during hydrolysis. Lignin is considered to be complicated species among the other species .i.e. cellulose and hemi-cellulose. It is vastly branched and three-dimensional structure. The basic unit of lignin is polyphenolic element and bonded by various hydroxyl, methoxy or phenylpropane units. The further subclasses of phenylpropane units includes sinapyl, p-coumaryl and coniferyl structures(Yun Yu 2008)

The intra linkage between units is dominated by ether bonds. The other intra bonding of lignin is covalent link, which intensify the adhesive property between lignin and its cellulose fiber called “potting matrix”. The molecular structure of lignin is demonstrated below(Dinesh Mohana 2006):

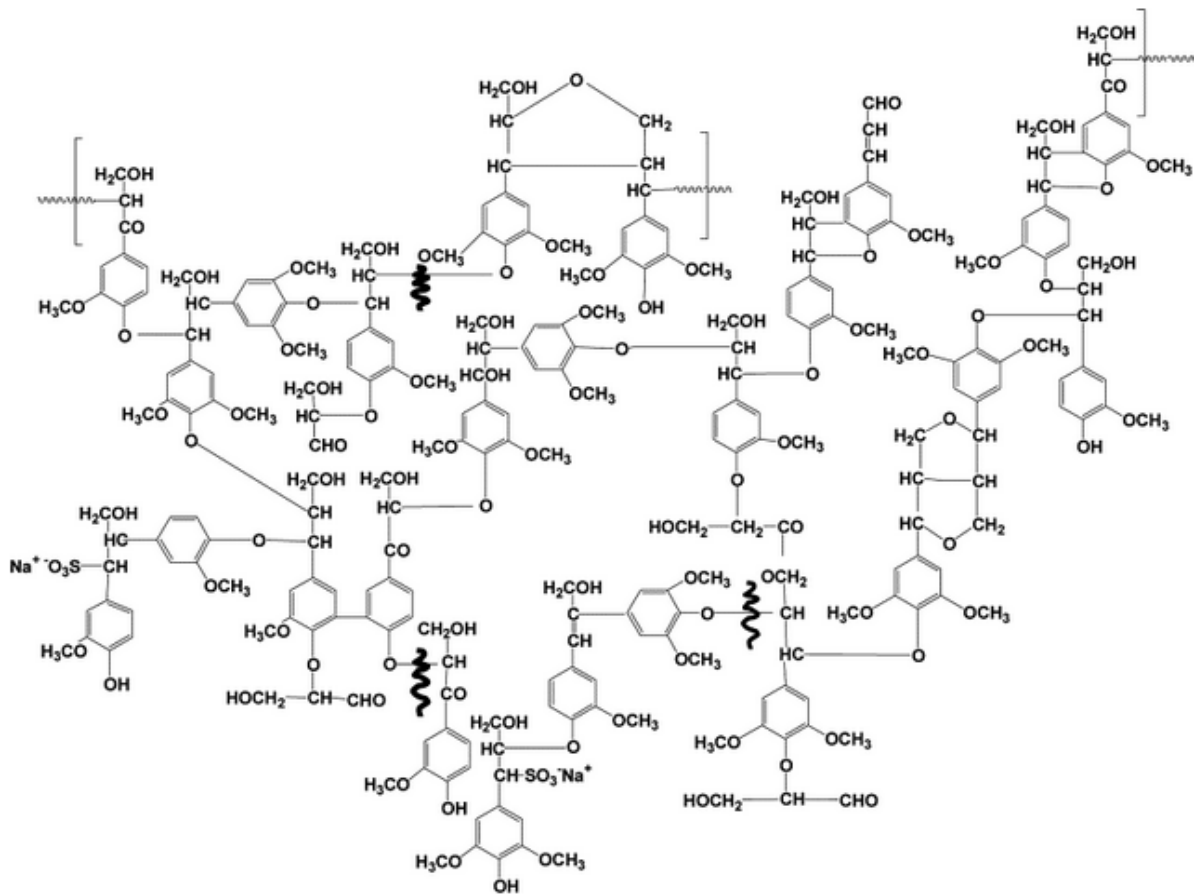


Figure 4 Lignin molecular structure

## 2.2 Micro-Reactor

Micro-reactors belong to one of great area of concern for researchers in today's world. The applications and implementation of novel chemical engineering concepts make micro-reactor a viable unit. It modifies the area to volume ratio which facilitates in mixing. Mixing through the micro-reactor is mainly dominated by laminar flow (Simon Dreher 2009). Another key element in micro-reactor is heat exchange efficiency. The heat exchange efficiency enables us to perform high exothermic reactions under isothermal condition. As a result, the unwanted reactions are suppressed inside the system. The parameters controlling in micro-reactors as compared to conventional reactors is better because of high surface to volume ratio(Jaehoon Choe 2003). The last key element is safe operating process; as mentioned before that the high exothermic reactions could be performed in well controlled conditions. (Prof. Dr. Peter H. Seeberger ,

Matlosz 2001). In figure 5, the mixing behavior in micro system is shown, normally in large scale the mixing is governed by turbulent regime. In case of laminar regime, the distance must be reduced so that molecules could diffuse into each other and good mixing is achieved even in laminar flow. To understand mixing quality, UV-VIS spectroscopy is utilized below(Anil R. Oroskar 2001):

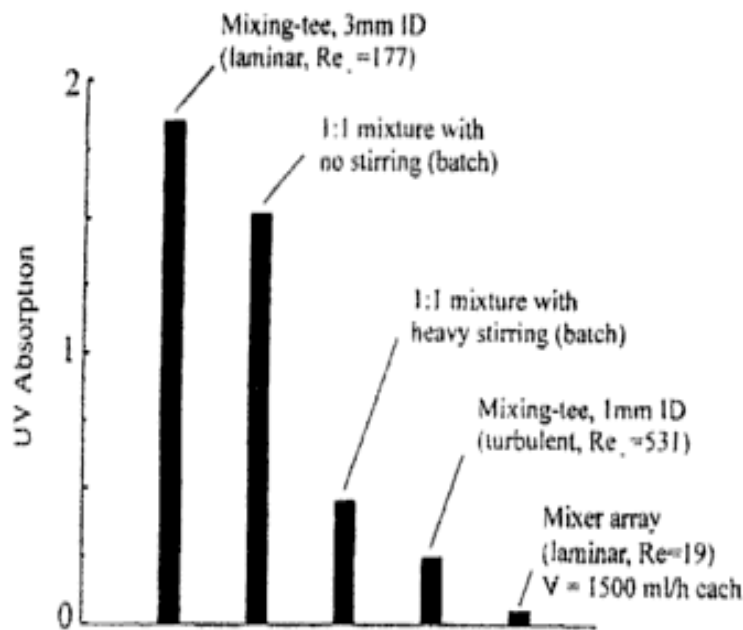


Figure 5 comparison between micro-reactor and conventional reactor mixing.

### 2.3 Super-Subcritical Water and Its Importance in Liquefaction Process.

The thermodynamic properties of liquid water changes with temperature, due to disturbance of hydrogen bonding(Scheraga 1962). At critical point of phase equilibrium the water properties for instance: density, thermal conductivity and viscosity are controlled by temperature and pressure(Takafumi Aizawa 2007). The fluid becomes non-polar, highly reactive and miscible for organic components; as a result water at elevated temperature works as a catalyst (Cai Y. Maa 2011). The Non-polar behavior of water is obvious; according to (Masato Morimoto 2012) dielectric constant of liquid water at 25 °C and 0.1MPa is 78. Whereas at 440 °C and 25-35MPa is 1.43-3.15(Table 1), therefore it decreases with density of water. The thermodynamic property of super and subcritical water is likely equivalent to acetone that makes solvent epitome to

reactive with organic component. Table 1 describes the thermodynamics properties of water as a function different temperature.

Table 1 physical properties of water

	Normal water	Subcritical water		Supercritical water	
Temp. ( $^{\circ}\text{C}$ )	25	250	350	400	400
Pressure (MPa)	0.1	5	25	25	50
Density, $\rho$ ( $\text{g cm}^{-3}$ )	1	0.80	0.6	0.17	0.58
Dielectric constant, $\epsilon$ ( $\text{F m}^{-1}$ )	78.5	27.1	14.07	5.9	10.5
Ionic product, $\text{pK}_w$	14.0	11.2	12	19.4	11.9
Heat capacity $C_p$ ( $\text{kJ kg}^{-1}\text{K}^{-1}$ )	4.22	4.86	10.1	13.0	6.8
Dynamic viscosity, $\eta$ (mPas)	0.89	0.11	0.064	0.03	0.07

The water separates into  $\text{H}^+$  and  $\text{OH}^-$  ions; however these ionic products are reversible and tend to be in equilibrium instantly because of the high reactivity. The reaction mechanism of biomass must be favored by ionic reactions because of the increased solubility in sub and supercritical water. The ionic product of water reacts with hydrocarbons chain and dissociates the chain, as a result hydrolysis reactions occurs. Furthermore there is also a possibility of condensation and cleavage reactions too. The lignocellulose biomass is vindicated to be highly influenced by sub or supercritical water. In such type of case, the water acts like reactant and catalyst and generates an additional pathway that produces oil. The biomass is dissociated and reformed by the action of  $\text{H}^+$  ions. The  $\text{H}^+$  of water ruptures the intra H-C chain into smaller fragments and later reform back the fragmented H-C chain to produce oil. It could be concluded that, sub-supercritical water provokes number of ionic reactions which are either acidic or basic nature to derive the biomass reaction rather than driving it via heat (Zhang 2010). Based upon above explanation, the hydrothermal liquefaction is more promising for direct conversion of biomass into bio-oil than the pyrolysis and other process, which does not contain water as solvent. The figure 6 shows the water properties as a function of temperature:

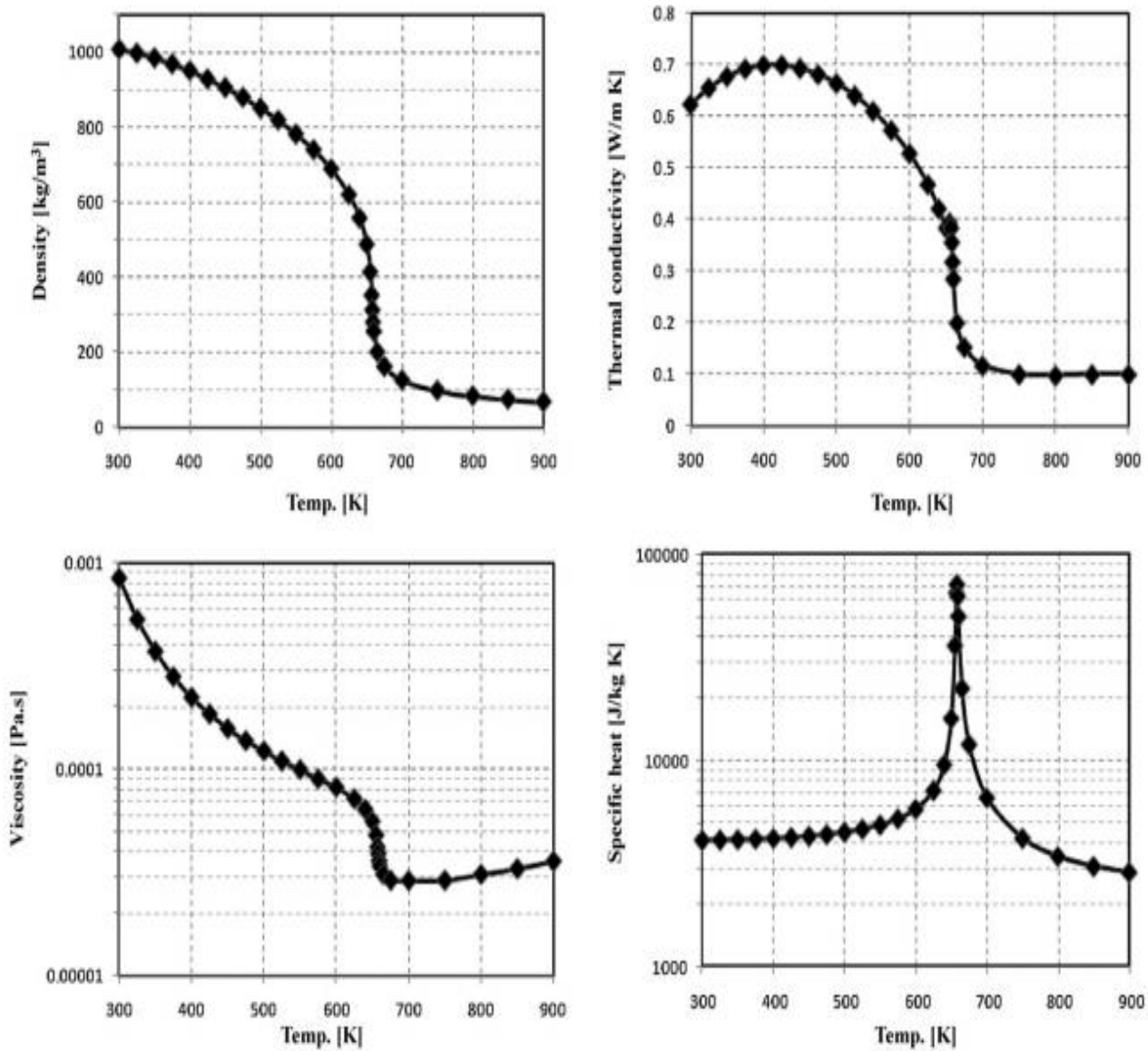


Figure 6 Thermodynamic properties of water as a function of temperature at 25MPa(Pooya Azadia 2011)



## 2.4 Biomass Conversion Techniques for Energy Applications

The conversion techniques of biomass is divided into two classes; biochemical and thermochemical conversion(Yokoyama 1993). According to (D. Humbird and D. Hsu 2011) the biochemical process consists of pre-treatment of biomass along with enzymatic hydrolysis for the residues of cellulose, then fermentation which gives glucose and xylose to ethanol. In biochemical the main products are ethanol and biogas. The yield is affected by composition of raw materials especially with the ratio of cellulose and lignin(McKendry 2002).

In general, thermochemical conversion (TCC) is also known as reforming process, where biomass is heated under pressurized and oxygen deprived enclosure. The long hydrocarbon chain of organic compounds (biomass) breakdown into shorter chain and produce syngas or oily liquid(Zhang 2010). TCC is divided into combustion, gasification, pyrolysis, carbonization, hydrothermal gasification and hydrothermal liquefaction.

Combustion is a process that generates heat, luminescence and exothermic reactions; which are complex homogeneous and heterogeneous reactions. The phenomena in combustion process are complicated; it includes diffusion heat conduction, radiation, convection, evaporation and mixture. During drying process in combustion the moisture is evaporated at less than 373K. This is an energy consumption process which lowers down the temperature inside the combustion chamber as showed in figure7 (Nussbaumer 2003). The environmental aspect of combustion is not favorable; it includes formation of  $\text{CO}_2$ ,  $\text{SO}_x$ ,  $\text{NO}_x$ , ozone and  $\text{NO}_2$  in ambient air.(Koppejan 2008).

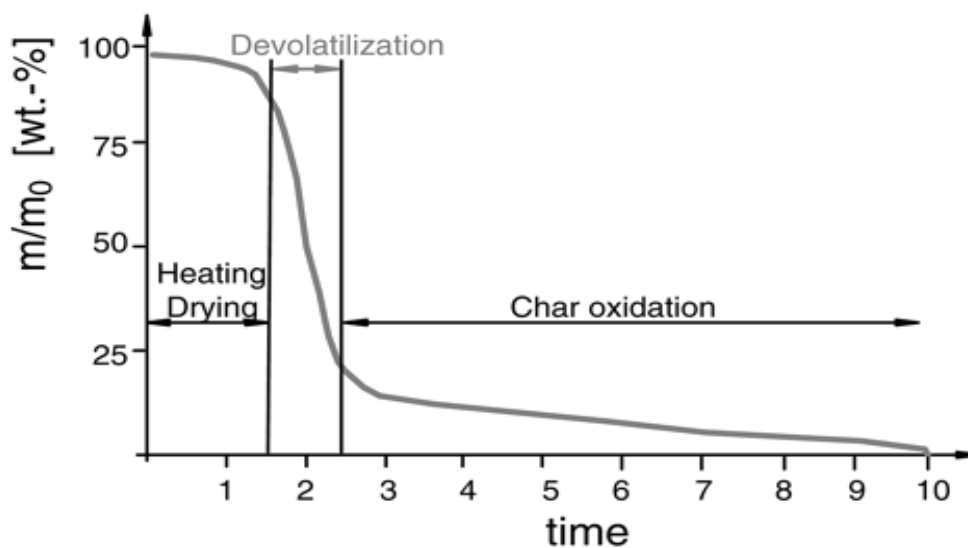
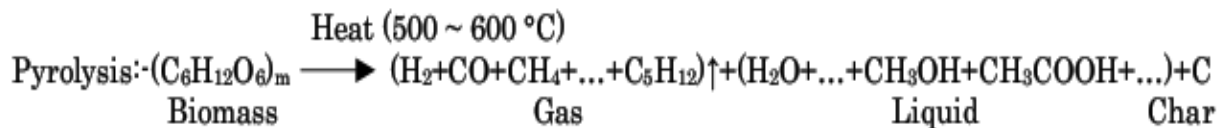


Figure 7 the combustion of biomass particles as a function of time

The gasification process produces hydrogen and carbon monoxide; which is also known as syngas, these syngas needs to be reformed in the bio-refineries. The operating conditions are more severe than pyrolysis, the temperature is above 1073K and the reaction is performed in the presence of oxygen. The gasification agents here are mainly air, oxygen, carbon-di-oxide and water; they are used in adequate mixture.

Pyrolysis is also thermal degrading process of biomass which directly produces syngas and oil. Both gasification and pyrolysis require dried biomass as feedstock, and the processes occur in an environment higher than 873K. Depend upon operating conditions and residence time; the pyrolysis process is further classified into slow and fast pyrolysis(Bridgwater 2012). The simple reaction of pyrolysis process is elucidated below:



Carbonization is used to produce charcoal mainly, when biomass is subjected to heating at 673K to 873K. The products of carbonization are mainly pyrolygneous acid, tar and combustible gases. In hydrothermal gasification process, the biomass is treated with hot compressed water. The temperature of water is above 648K and pressure 20MPa, the state of water is mainly gaseous (supercritical water). The dielectric property of water at that temperature precedes the dissociation of biomass(Yokoyama 2008). The figure 8 illustrates the classification of thermochemical conversion of biomass.

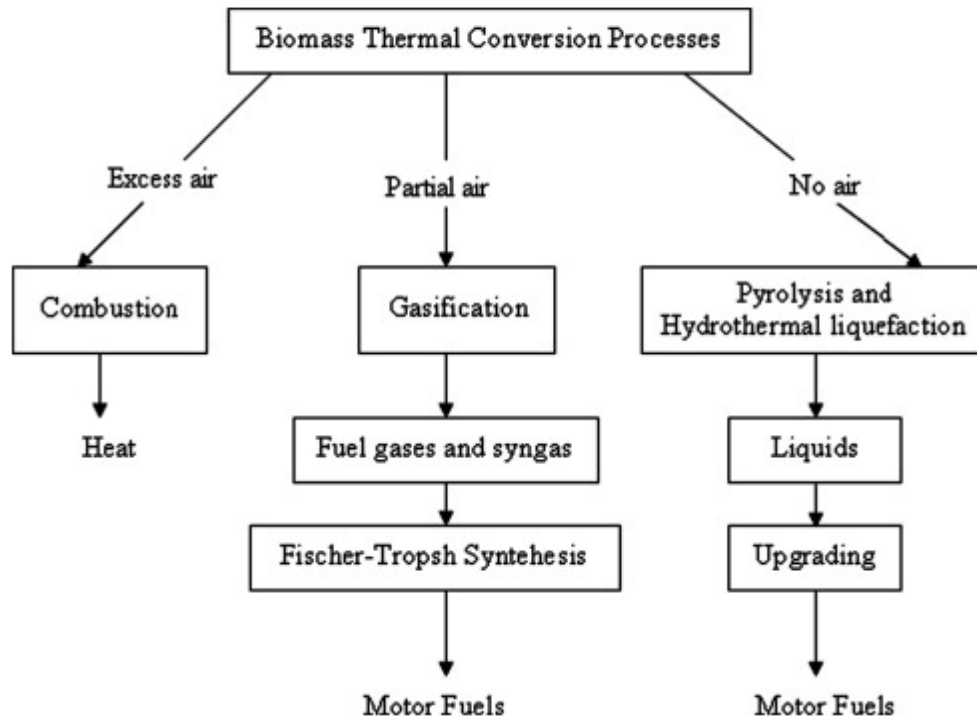


Figure 8 the thermochemical conversion of biomass(Mustafa Balat 2009)

#### 2.4.1 Hydrothermal Liquefaction Process (HTL)

The hydrothermal liquefaction is synonym to hydrous pyrolysis. HTL dissociates the complicated organic components into products; for instance bio-crude oil, gas and other hydrocarbon chains. In this process, the biomass is subjected to subcritical water at temperature 573-623K and pressure of 13-20MPa, showed in figure9 below. At that pressure and temperature the reactivity of water is high and water works as catalyst. The continuous medium (water) ruptures the internal structure of biomass and breaks molecules into small H-C chains. If the reactivity and rate of reaction is low, we may needs to add a catalyst. The Hydrothermal process does not contain drying step, whereas in gasification and pyrolysis process the drying is essential (Zhang 2010). The product from HTL contains high energy contents compare to pyrolysis process because most of the oxygen is converted into carbon dioxide in the hydrothermal liquefaction process. According to (DTI 2006), the oxygen contents in HTL is 10–15 by weight percent, however in pyrolysis it is 35–40 wt%. In addition, HTL bio-oil has 30–35 MJ/kg heating value (Frans Goudriaan 2006), which is greater than pyrolysis bio-oil (16–21 MJ/kg) (Silvia Vivarelli 2004).

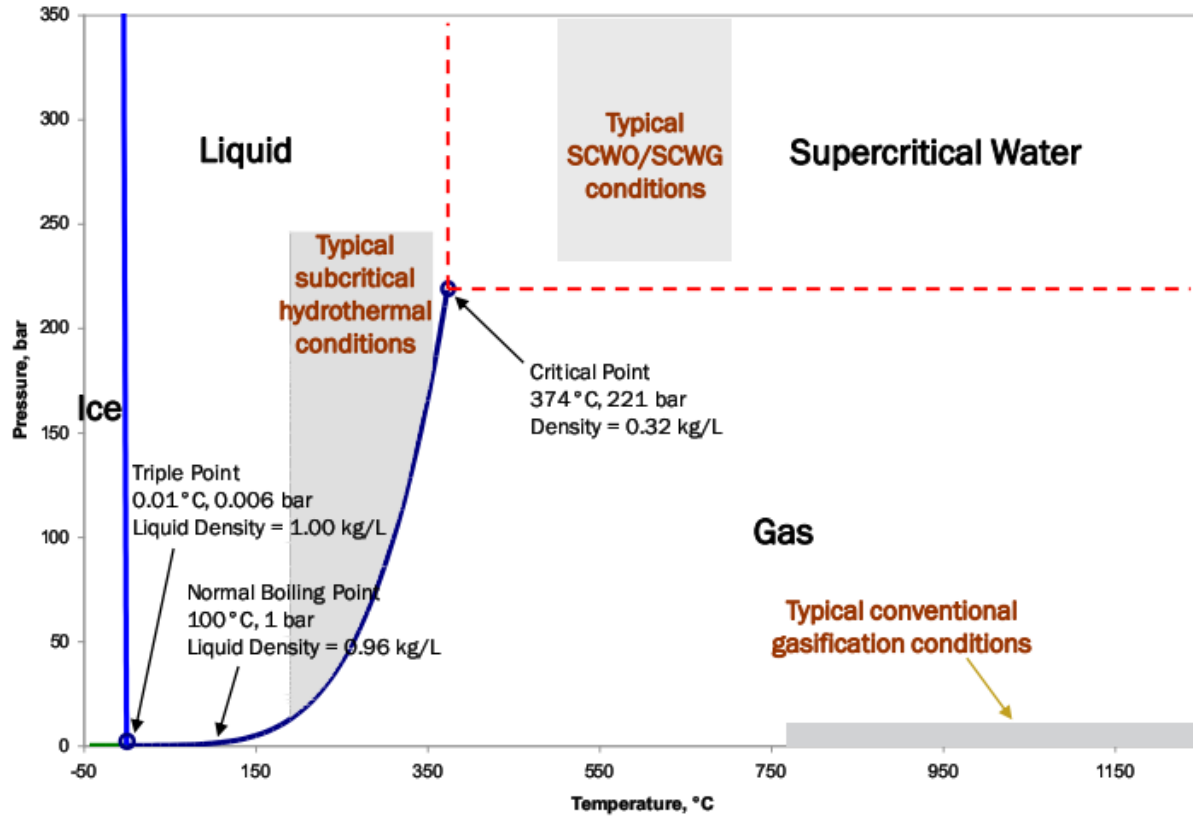


Figure 9 phase diagram of water, indicating operating conditions of hydrothermal liquefaction

## 2.5 Kinetic Model

Many researchers (Zhang, Huang et al. 2008, D. Knez evic´ 2009, Zhang, Huang et al. 2012) have used lumped kinetics to define the reaction pathway of biomass. In most of the cases the rate of reaction is well defined by Arrhenius equation; which is the function of temperature. The Arrhenius equation is illustrated below:

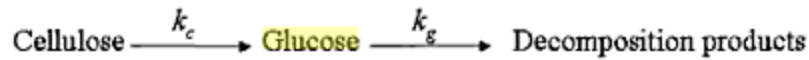
$$k = A * \exp\left(\frac{-E_i}{RT}\right) \quad (1)$$

$$\ln k = -\frac{E_i}{R} * \frac{1}{T} + \ln * A \quad (2)$$

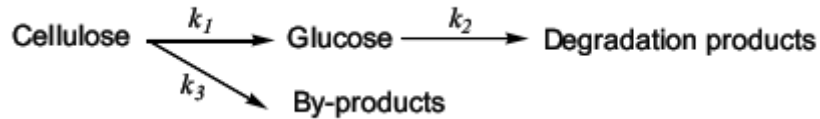
In equation 1; k is the rate of reaction, 'A' is pre-exponential factor and  $E_i$  is the activating energy. The equation 2 is the linearized form; the plot of reaction rate constant [ $\ln k$ ] at different temperature [ $1/T$ ] should be linear to give Arrhenius parameters.

### 2.5.1 Kinetic Model of Cellulose

Cellulose produces glucose and by-product at subcritical and supercritical water in continuous tubular reactors. The reaction pathway of cellulose is found to be consecutive and parallel. According to (Zhang 2008), the cellulose first dissolve and then it is hydrolyzed to product glucose . The Zhang work focused on glucose decomposition. The main decomposition products of glucose are fructose, laevoglucose, glyceraldehyde and erythrose. He defined the reaction rate constant [kg] which is 5.04 s<sup>-1</sup> at 573K.



For cellulose decomposition in subcritical water at 513-533K temperature; (Guang Yong Zhu 2011) reported that hydrolysis of cellulose consist of parallel reactions , where cellulose gives glucose and by-products. Until now, the research (Zhang and Guang Yong Zhu) have showed that the reaction pathways for the decomposition of cellulose in subcritical water is either consecutive or parallel reactions. The common reaction path of cellulose between Zhang and Guang is consecutive reaction.



In addition to cellulose decomposition in sub critical water, recently the (Olanrewaju 2012) performed experimental work for the kinetic parameters and proposed the rate constant at subcritical temperatures. In table 2, Olanrewaju elucidates the conversion of cellulose at different temperature and residence time. The ‘X’ is the conversion and ‘t’ is the residence time. The conversion of cellulose is 69.8% at residence time of 0.788s. Since Olanrewaju operating conditions are near to our case therefore we have taken his reaction parameters for cellulose. The more details about kinetic parameters are discussed in ‘Method of Study’ section.

Table 2 conversion of cellulose at subcritical temperature

270 °C		280 °C		290 °C		295 °C		300 °C		320 °C	
$\tau$	X	$\tau$	X	$\tau$	X	$\tau$	X	$\tau$	X	$\tau$	X
0.00	0.00	0.00	0.00	0.00	0.00	0.00	0.00	0.00	0.00	0.00	0.00
0.445	0.165	0.437	0.234	0.438	0.330	0.424	0.316	0.402	0.465	0.400	0.723
0.498	0.257	0.489	0.262	0.469	0.324	0.453	0.431	0.494	0.487	0.437	0.831
0.537	0.186	0.559	0.177	0.545	0.455	0.525	0.377	0.534	0.306	0.495	0.868
0.601	0.202	0.606	0.237	0.612	0.431	0.623	0.581	0.582	0.464	0.555	0.922
0.725	0.289	0.712	0.327	0.745	0.553	0.691	0.855	0.684	0.565		
0.877	0.342	0.832	0.402	0.870	0.631	0.808	0.691	0.788	0.698		

The differential equations of cellulose decomposition for consecutive reaction path are:

$$\frac{dC}{dt} = -k_1 * C$$

$$\frac{dG}{dt} = k_1 * C - k_2 * G$$

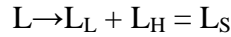
$$\frac{dD}{dt} = k_2 * B$$

Where C is cellulose, G is glucose and D is degraded by-products. The rate constants are denoted by k1 and k2.

### 2.5.2 Kinetic Model of Lignin

In hydrothermal liquefaction, the modeling of lignin is performed by (Zhong and Wei 2004, Zhang, Huang et al. 2008, Zhang, von Keitz et al. 2008, Zhang, Huang et al. 2012). The (Zhang, Huang et al. 2008) used Kraft pine lignin to describe the mechanism., according to them the reaction consists of fast and slow reaction from temperature 573-653K. Initially lignin is decomposed into soluble components (consist of low and high chain molecules) in 1minute

completely. Furthermore Zhang Huang describes that the reaction is done in slow momentum, where insoluble components (char) are produced by mean of condensation of soluble and insoluble species. The reaction path is mentioned below:



$L_L$  and  $L_H$  are low and high molecular components of lignin, whereas  $L_S$  is soluble lignin. The proposed Arrhenius parameter is  $E_a = 37 \text{ kJ/mole}$ . Zhang Huang concluded that lignin degradation is well defined by Arrhenius equation.

However (Matsumura 2012, Matsumura 2013) proposed the reaction path of lignin in Subcritical water as showed below.

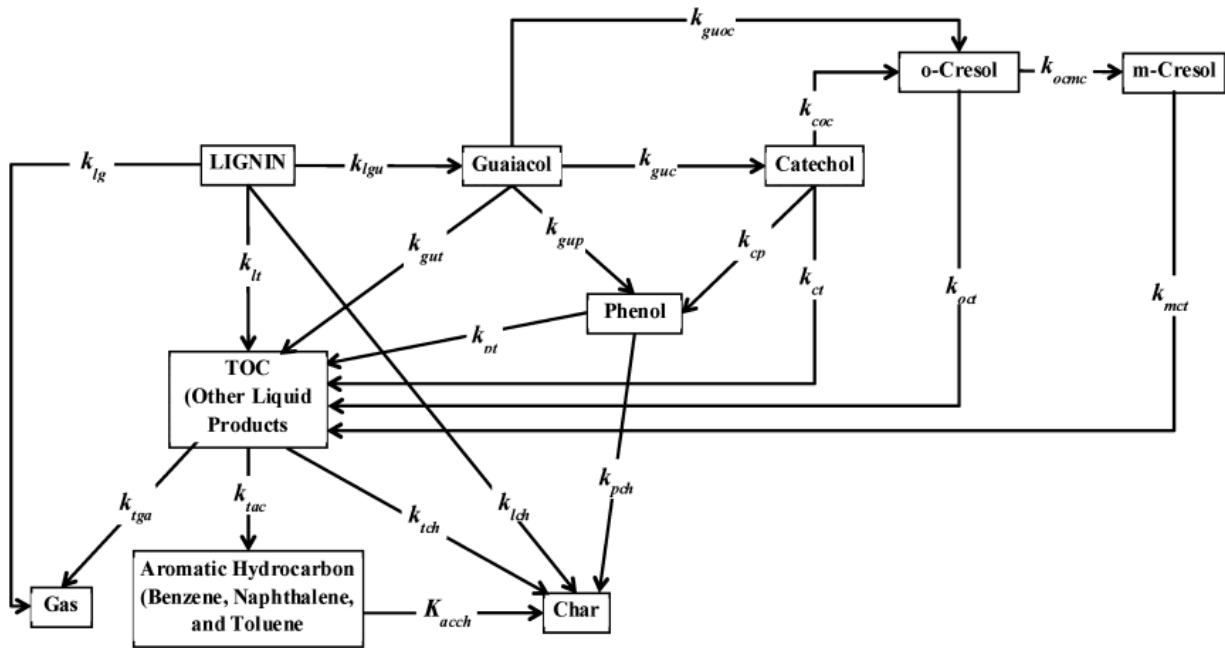


Figure 10 reaction path of lignin at subcritical water

Matsumura well describes the lignin degradation in subcritical water at 573-643K temperature and 25MPa pressure. The decomposed products of lignin are guaiacol, gas, TOC(other liquid products), aromatic hydrocarbon(benzene, naphthalene and toluene), phenol, char, catechol, 0-cresol and m-cresol. However Matsumura mentioned that the key products of lignin after decomposition are Total organic components (TOC), gas and char. For our studies, we have selected Matsumura reaction pathways and the opted rates constants at 573K. The rate constant for lignin to TOC is  $6.35 \times 10^{-1}$ , lignin to gas is  $3.65 \times 10^{-2}$  and lignin to char is  $2.03 \times 10^{-1}$ . The proposed

Arrhenius parameter is 43.15kJ/mole. For our convenient, we are assuming rate constants for lignin (L) to TOC (T) is  $k_1$ , lignin to gas (G) is  $k_2$  and lignin to char (C) is  $k_3$ . The differential equations are:

$$\frac{dL}{dt} = -k_1 * L - k_2 * L - k_3 * L$$

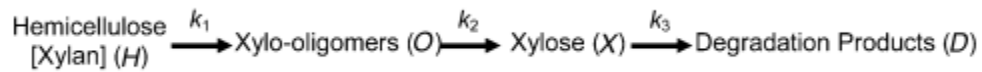
$$\frac{dT}{dt} = k_1 * L$$

$$\frac{dC}{dt} = k_2 * L$$

$$\frac{dG}{dt} = k_3 * L$$

### 2.5.3 Kinetic Model of Hemi-cellulose

The decomposition of hemi-cellulose in pressurized low polarity water in tubular flow through reactor is studied by (Mazza 2010). He defined two paths of hemi-cellulose decomposition which are mono and bi-phase reaction path. However experimentally it is vindicated that reaction path is mono-phase, which is shown below:



The set of differential equations are:

$$\frac{dH}{dt} = -k_1 * H$$

$$\frac{dO}{dt} = k_1 * H - k_2 * O$$

$$\frac{dX}{dt} = k_2 * O - k_3 * X$$



$$\frac{dD}{dt} = k_3 * X$$

Where H denotes hemicellulose, O is xylose-oligomers, X is xylose and D is degraded products. The rates of reactions are defined as  $k_1$ ,  $k_2$  and  $k_3$ .

Mazza defined the rate constants at 423-443K temperature, the conversion of hemi-cellulose is 50% in 5minutes residence time; both temperature and residence times are far away with ours current studies. Therefore the kinetic model for hemi-cellulose for ours system could not be selected.

Furthermore, the evaluation of rate constants proposed by Mr.Mazza reveals that, they are not dependent or well defined by Arrhenius equation because of non-linear Arrhenius plots, showed in appendix A. According to equation 2 of kinetic model in 2.2, the behavior of  $[\ln k]$  and  $[1/T]$  must be linear to predict Arrhenius parameters and use these parameters for any desirable temperatures and other operating conditions.

## 2.6 Turbulence Model

The two equations k-epsilon ( $k-\epsilon$ ) turbulent model is considered because the flow in micro-reactor varies from laminar to turbulent(S.Moussiere 2007). Turbulence is one of the characteristics of fluid motion in which eddy formation (void spacing) takes place because of irregularity of the fluid. This behavior normally happens at high Reynolds number of the flow. *The turbulence model is a computational procedure to close the system of mean flow equations (Bakker 2002)*, therefore it is also very important to know that how the mean flow affected by turbulence. The sum of the mean kinetic energy and turbulent kinetic energy can be known as instantaneous kinetic energy. The k-epsilon model mostly put emphasis on mechanism by which turbulent kinetic energy can be affected. This model has some practical advantages for instance ease of implementation, facilitate in convergence of calculations, reliable predictions for fluid. Contrary to that, it has some cons to for instance the model calculates only valid fluid, sometimes it tends to have unreliable prediction especially in jet flow, strong separation, immense swirling or rotational flows(D.M. Hargreaves 2007). The application of k-epsilon model has wide applications in different fields of engineering. It applies to wind, chemical, energy, material &

science, process and mechanical engineers. The transport equation of standard k-epsilon model is:

$$\frac{\partial}{\partial t}(\rho k) + \frac{\partial}{\partial x_i}(\rho k u_i) = \frac{\partial}{\partial x_j} \left[ \left( \mu + \frac{\mu_t}{\sigma_k} \right) \frac{\partial k}{\partial x_j} \right] + G_k - \rho \epsilon + S_K$$

$$\frac{\partial}{\partial t}(\rho \epsilon) + \frac{\partial}{\partial x_i}(\rho \epsilon u_i) = \frac{\partial}{\partial x_j} \left[ \left( \mu + \frac{\mu_t}{\sigma_\epsilon} \right) \frac{\partial \epsilon}{\partial x_j} \right] + C_{1\epsilon} \frac{\epsilon}{k} G_k - C_{2\epsilon} \rho \frac{\epsilon^2}{k} + S_\epsilon$$

Where 'k' is turbulent kinetic energy and epsilon 'ε' is turbulent dissipation rate. S<sub>K</sub> and S<sub>ε</sub> are the source term; G<sub>k</sub> is produced kinetic energy because of mean velocity gradient. The μ<sub>t</sub> is turbulent viscosity, ρ is the density and the model constants are C<sub>1</sub>=1.44, C<sub>2</sub> = 1.92 σ<sub>k</sub>= 1.0 and σ<sub>ε</sub>=1.3.(Prof. Dr. Uwe Riedel 2011)

## 2.7 Reynolds Number of the Flow

The k-epsilon model as mentioned above ensures stability in the system when the flow is between laminar and transient. The hydrothermal process of biomass lies between laminar and turbulent flow(Hendry 2012) . (Pooya Azadia 2011) calculated the Reynolds number of the fluid to know the behavior of the flow inside the system. The Reynolds number of the flow could be calculated by:

$$N_R = \rho * U * d_h / \mu$$

Where ρ= density in kg/m<sup>3</sup> , U is velocity in m/s ,d<sub>h</sub> is hydraulic diameter(m) of the pipe and μ is absolute or dynamic viscosity in N.s/m<sup>2</sup> (Allen 1996).

## 2.8 Turbulence Intensity (T.I)

Practically it is observed that the importance of T.I is vital for prediction of the flow. The core purpose is to avoid back flow problem. The back flow mainly happens at flow inlets and outlet, therefore T.I needs to be defined as boundary conditions of the system. T.I value is in percent when 1 is the lowest and 10 is the highest. (CFD-Online). 'Re' is the Reynolds number and d<sub>h</sub> is hydraulic diameter (inlet diameter).

$$T.I = 0.16 Re_{DH}^{-1/8}$$

## 2.9 Multiphase Model

The software ANSYS fluent provides a wide range of multiphase model, which are mixture model, Eulerian model, and volume of fluid (VOF) model. Based upon case to case the application of these models varies. The VOF is basically for large surface area of disperse phase for instance floating oil on water. Whereas the Eulerian and mixture are almost same, the basic difference is that the mixture model use segregated solver for ease phase and solidification problems could not be modeled. However Eulerian model could use segregated and coupled solver both but it needs more computational resources than mixture model and sometimes it has problem related to convergence of the solution due to instability. Therefore the selected model is mixture multiphase model.

The mixture model is a multiphase model and has better convergence properties. It is easy to implement as compare to Eulerian Model. The stability of mixture model is better than Eulerian model and it solves most of the engineering problem concerning to multiphase. It is applicable with phases at different velocities and if the velocities are same then mixture model consider the fluids as single phase. This model simulates fluid or particle and solves momentum, energy, and continuity equations for mixture. It also solves volume fraction equations for secondary phase and algebraic expression for relative velocities.

The single phase approach is being used by mixture model; the two main benefits are: allows phases to be interpenetrated, second it uses slip velocities for phases moving at different velocities. The range of volume fraction for secondary phases is from 0 to 1. The application of Mixture model included particle laden flow; where particles move with continuum phase, cyclone separator, and bubble flow (guide 2010)

### 2.9.1 Continuity Equation of Mixture Model

$$\frac{\partial}{\partial t}(\rho_m) + \nabla \cdot (\rho_m v_m) = 0$$

$v_m$  is mass average velocity:

$$v_m = \sum_{K=1}^n \alpha_K \rho_K v_K / \rho_m$$

$\rho_m$  is the mixture density

$$\rho_m = \sum_{K=1}^n \alpha_K \rho_K$$

$\alpha_k$  is volume fraction of phase k,  $\rho$  is the density, n is the number of phases and v is the velocity.

### 2.9.2 Momentum Equation of Mixture Model

The momentum equation for all phases is:

$$\frac{\partial}{\partial t}(\rho_m v_m) + \nabla \cdot (\rho_m v_m v_m) = -\nabla p + \nabla \cdot [\mu_m (\nabla v_m + \nabla v_m^T)] + \rho_m g + F + \nabla \cdot \left[ \sum_{K=1}^n \alpha_k \rho_k v_{dr,k} v_{dr,k} \right]$$

Where n is the number of phases, F is body force and  $\mu_m$  is mixture viscosity.

$$\mu_m = \sum_{K=1}^n \alpha_k \mu_k$$

$v_{dr,k}$  is the drift velocity for disperse phase k, it is equals to  $v_k - v_m$

### 2.9.3 Energy Equation of Mixture Model

For mixture the equation of energy could be elucidated as:

$$\frac{\partial}{\partial t} \sum_{K=1}^n (\alpha_k \rho_k E_k) + \nabla \cdot \sum_{K=1}^n (\alpha_k v_k (\rho_k E_k + p)) = \nabla \cdot (k_{eff} \nabla T) + S_E$$

$K_{rjf}$  is effective conductivity ( $\sum \alpha_k (K_k + K_t)$ ),  $S_E$  is the volumetric heat source.

### 2.9.4 Relative (slip) Velocity and Drift velocity

$$v_{pq} = v_p - v_q$$

Where  $v_p$  and  $v_q$  are the velocities of secondary and primary phases.

The drift velocity is:  $u_k^r = u_k - u_m$ .

### 3 Method of Study

#### 3.1 General

Computational fluid dynamic (CFD) modeling is done to simulate the biomass liquefaction process by sub/supercritical water in a tubular micro-reactor. CFD is used to predict the operating conditions, physical properties, residence time and optimum conversion yield. In CFD; we have used ANSYS fluent simulation software for fluid dynamics and ANSYS gambit for meshing & geometry. The core purpose of using CFD is to optimize the operating conditions and to visualize the output parameters.

The 2-Dimensional geometry is created in ANSYS gambit to save computational resource. The constructed geometries are imported into ANSYS fluent software for fluid dynamics. The solution is not dependent upon mesh i.e. convergence is improved by mesh refinement. The further details and quality of geometry is discussed in (3.2). The pressure-based solver is used in ANSYS fluent to solve the momentum, energy, species transport and continuity equations. The SIMPLEC/SIMPLE algorithm is considered for the coupling of pressure-velocity. The order of discretization schemes is first and second for reliable prediction of continuity, momentum, species and energy equations. The under-relaxation factor for species is 0.95 to facilitate the convergence, however later they have been changed to 1. The under-relaxation for rest of the equation is 1.

The boundary conditions for all inlets are velocity based and for outlet it is pressure based. By experience we know that velocity-pressure combination give stable results. The convergence criterion is  $10e-3$  for continuity residues. The turbulence model k-epsilon (discussed in 2.6) is used for turbulence. The turbulent intensity (discussed in 2.8) as a function of inlets and outlets opening diameter is considered. The multiphase model Mixture Model (discussed in 2.9) is being considered. For temperature gradient inside the system, the energy equation is enabled.

The thermo-physical properties of water for instance viscosity, conductivity and density as a function of temperature is considered. In ANSYS fluent, these properties are introduced via piece-wise and polynomial.

Water viscosity coefficient is  $0.00527-2.45 \cdot 10^{-5} \cdot T+3.83 \cdot 10^{-8} \cdot T^2-1.97 \cdot 10^{-11} \cdot T^3$  .

Water conductivity coefficient is  $-2.596+0.0195 \cdot T-3.44 \cdot 10^{-5} \cdot T^2+1.80 \cdot 10^{-8} \cdot T^3$

The model components for biomass (discussed in 2.1) are cellulose, lignin and hemicellulose. The constant densities of model components are 1500kg/m<sup>3</sup>, 1520kg/m<sup>3</sup> and 1800kg/m<sup>3</sup>. The molecular weight of cellulose and hemicellulose and are 162g/mole, 132g/mole and for lignin it is assumed to be 260g/mole(Goring , Q.Hu 2002, Blokhin, Voitkevich et al. 2011, Zhang, Tu et al. 2011). The average weight and average density of model component for biomass is 184g/mole and 1606 kg/m<sup>3</sup>. The temperature of biomass solution is 323K and for supercritical water it is 647K with pressure 20MPa.

### **3.2 Selection and Construction a Physical Model**

For physical model, initially the geometry of different dimensions is constructed in ANSYS gambit software version 2.4.6. Special consideration is given at inlets and outlet boundaries by mean of decreasing mesh size. In order to save computational resources we have chosen 2D geometry. In two dimensions the XY coordinates are considered and Z-axis is equal to zero. Cai Y.Maa (Cai Y. Maa 2011, Cai Y. Ma 2012) uses 2D geometry for jet reactor and tubular heat exchangers, though both cases are complicated, the results are satisfactory and reasonable. The mesh size and spacing plays integral role on the simulated results therefore we have given considerations on it while making geometry. The key quality parameter of mesh is orthogonal quality; 0 is (worst) and 1 is (best). It is a thumb rules that a good geometry leads to good simulation.

The biomass solution is diluted 5% by weight. Since the water is predominated in the system, therefore the substrate is incompressible flow (Yoshio Masuda 2006). The velocity of biomass solution and critical water is varied from 0.1-0.5 m/s and different combination of velocities is studied with different geometries. In addition, the effect of double inlets and inlets diameter are also examined.

### **3.3 Modeling for Reactor Containing Particles**

All the physical and thermodynamic properties introduce for feed and reactor are remained same in this task. Few changes have been made in the biomass concentration, which is increased from 5% to 10% by weight. The different velocity of biomass solution and supercritical water is studied. For particles movement inside the system, we have used weightless particle. That weightless particle is introduced from center position of biomass inlet. The interaction of weightless particle with continuous medium is enabled. The drag law is spherical and unsteady

particle tracking is enabled too in ANSYS fluent. The particle injection type is single whereas the stop time(s) is 100 to make the iteration till end. The physical model related to particle is not selected because the particle is weightless. The default value for maximum number of steps is chosen which is 500 also by default step length factor is 5. The number of continuous phase iterations is 10.

### 3.4 Modeling of Reaction

The modeling of model components i.e. cellulose, hemi-cellulose and lignin is done by ANSYS fluent and MATLAB. In fluent software, the finite rate species transport model is considered because the rate of reaction is well defined by Arrhenius equation. The finite rate transport model requires stoichiometry coefficient and rate exponent of each chemical species along with Arrhenius parameters. These stoichiometry coefficients and rate exponents could not be found in any paper related to hydrothermal liquefaction reactions; therefore we assume the value be 1 for stoichiometry coefficients and rate exponents.

In MATLAB, the equation 1(see 2.5) for Arrhenius equation is model. The developed codes and functions files of MATLAB are attached in the Appendix E. For cellulose; the activating energy is 97.5E03 and pre exponential constant is 10E08. For the glucose decomposition to degraded products; the rate constant is 5.04s<sup>-1</sup>. For lignin; the rate constants from lignin to TOC is 6.35E-01, lignin to char is 2.03E-01 and lignin to Gas is 3.65E-02. The conversion of model components is calculated by:

$$X_i = \left( \frac{W_{0i} - W_i}{W_{0i}} \right) * 100$$

X is the conversion in percentage, W<sub>0</sub> is the total amount, W is the recovered amount (residue) and 'i' is the number of components.

### 3.5 Modeling of Real Biomass Particles

Particle size of real biomass is a challenging task, and its importance is dominant in the system. We simulated different particle size from 5 to 1000 microns in ANSYS fluent. The considered particle is spherical in shape with inert properties. The particle is interconnected with continuous medium to observe the real effect of continuous medium on disperse medium. The time per iteration is 0.001s for better results. The relative velocity of the particle is 0.2m/s, calculated by ANSYS fluent. The calculated density of particle is  $1606\text{kg/m}^3$  with feed percentage of 5% by weight. The skip factor is 5 for better visual illustration of particles in the system.



## 4 Results and Discussions.

### 4.1 Selection and Construction a Physical Model

#### 4.1.1 Geometry Construction

As mentioned before that 2-Dimensional geometry is made in ANS Gambit software. To examine the optimum behavior of the fluid, the different geometries are being constructed. The diameter of main body is varied from 1.8mm to 6mm, whereas the diameters of upper and lower inlets are varied from 1mm to 6mm. In figure 11&12, the important geometries are showed; remaining geometries which we examined during evaluation are mentioned in Appendix B. Initially we study the geometry of 1.8mm diameter (y-axis), 10mm length (x-axis) and 1mm upper inlet diameter.

Later on the inlet diameter is increased to 6mm (y-axis), along with upper and lower inlets of 1mm each. The length of the geometry is remained same .i.e.10mm in x-axis dimension. The type of mesh is TRI and QUAD, which is used in combination near boundary conditions. The density of mesh at boundaries is double ratio to ensure realistic fluid flow. The mesh density is controlled by single and double ratio. The overall quality of the geometry is admissible with orthogonal quality range of 0.73 on a scale of 1(best) and Aspect ratio of 7.29E-01. The solution convergence does not depend upon mesh refinement which shows that there are no miss or uneven distribution of mesh. The quality of geometries is mentioned below in table 3:

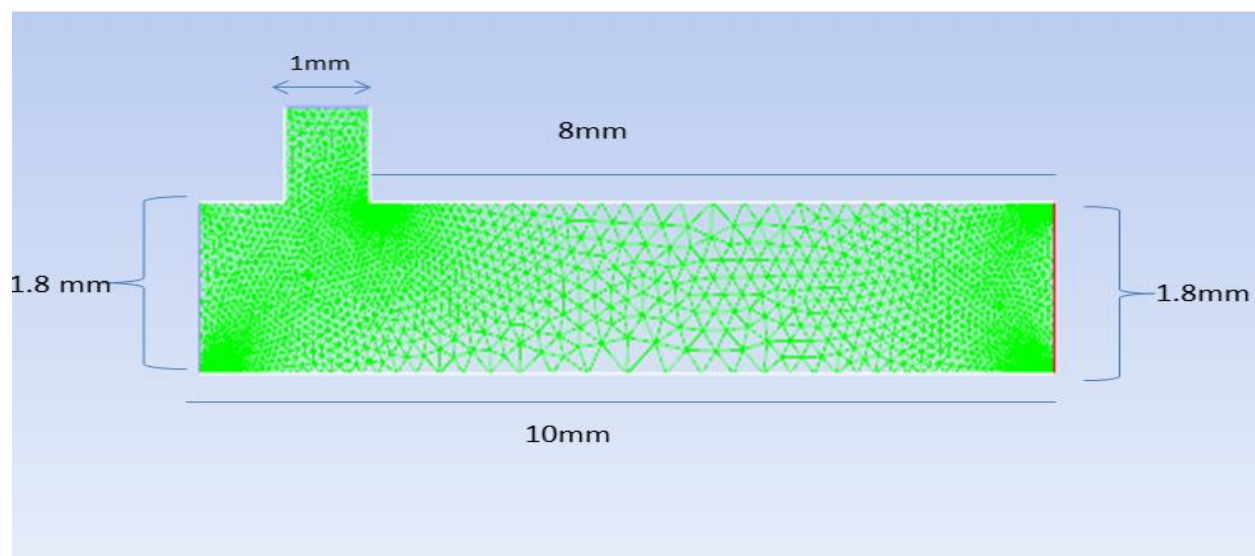


Figure 11 examined geometry of 1.8mm diameter.

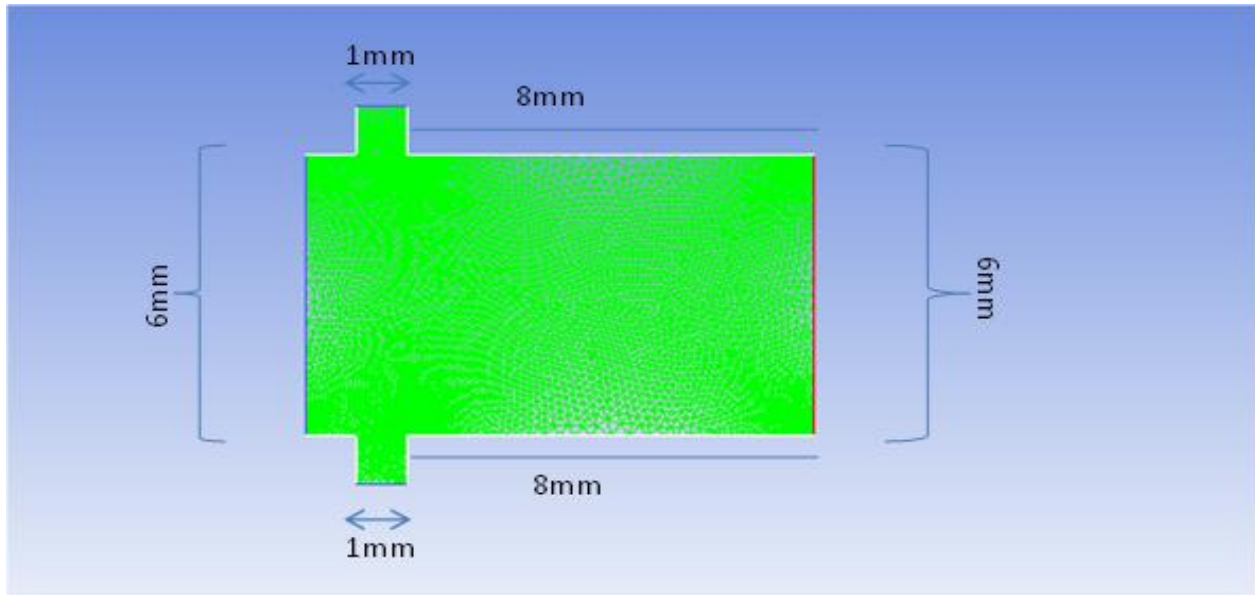


Figure 12 opted and developed geometry for our system.

Table 3 the quality parameters of geometry and mesh

Quality Parameters	
<b>Avg: mesh space</b>	0.22mm
<b>Velocity inlet mesh space</b>	0.3mm
<b>Velocity inlet2 mesh space</b>	0.1mm
<b>Ratio (inlet1 &amp; 2)</b>	1.1 double & 1.11 single
<b>Outlet</b>	Pressure outlet
<b>Maximum Aspect ratio</b>	7.29E-01
<b>Orthogonal quality range</b>	0.723

#### 4.1.2 Effect of Velocity on Outlet Temperature

The diluted biomass solution of 5% by weight and 95% of supercritical water is used. The velocity effect of biomass and critical water is studied. Initially, the velocity of biomass is kept constant whereas the velocity of supercritical water is varied. Later the velocity of water is constant and biomass velocity is changed. Figure 13, it is observed that as the velocity of biomass solution increase, the outlet temperature is governed by biomass temperature. This behavior is logical because the mass flow rate of biomass solution is increased too which suppresses the supercritical water flow downward; it is easily vindicated by blue large curve. Figure 14, when the velocity of supercritical water increases; the outlet temperature is mainly covered by critical water. The supercritical water wiped the biomass in upward direction; also some portion of biomass had backflow.

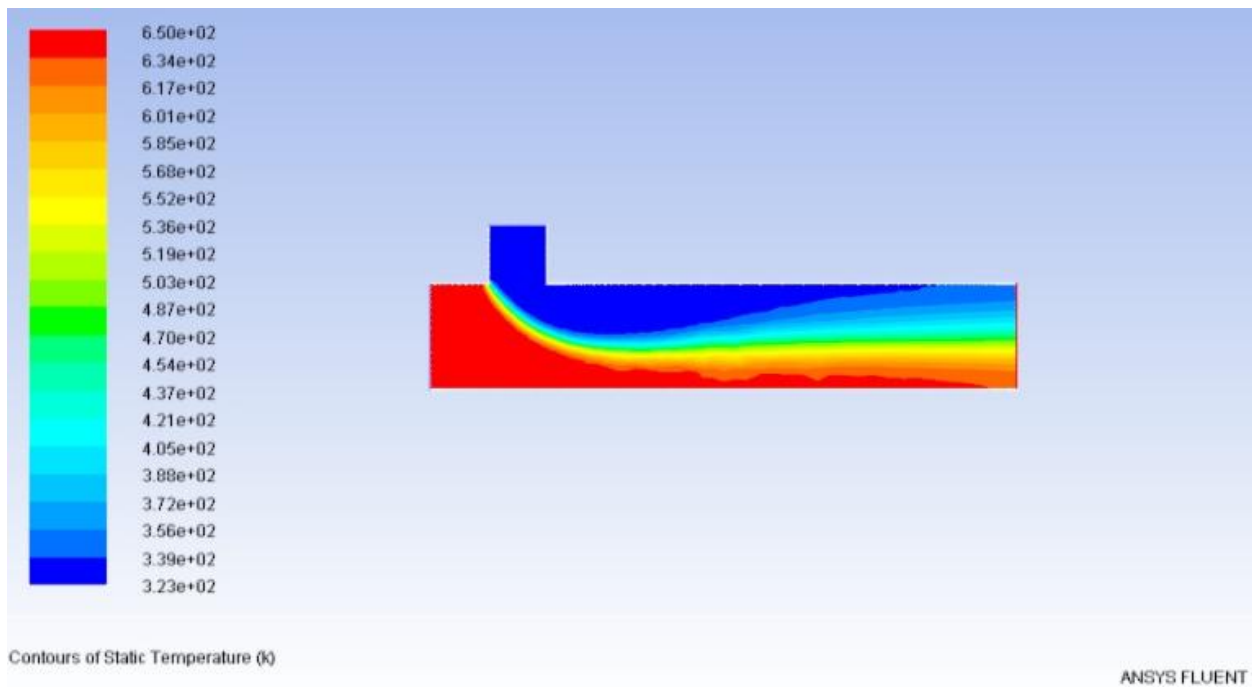


Figure 13 the biomass is introduced from upper inlet with 0.4m/s increased velocity, whereas the supercritical water is introduced from left hand side with low velocity of 0.3 m/s.

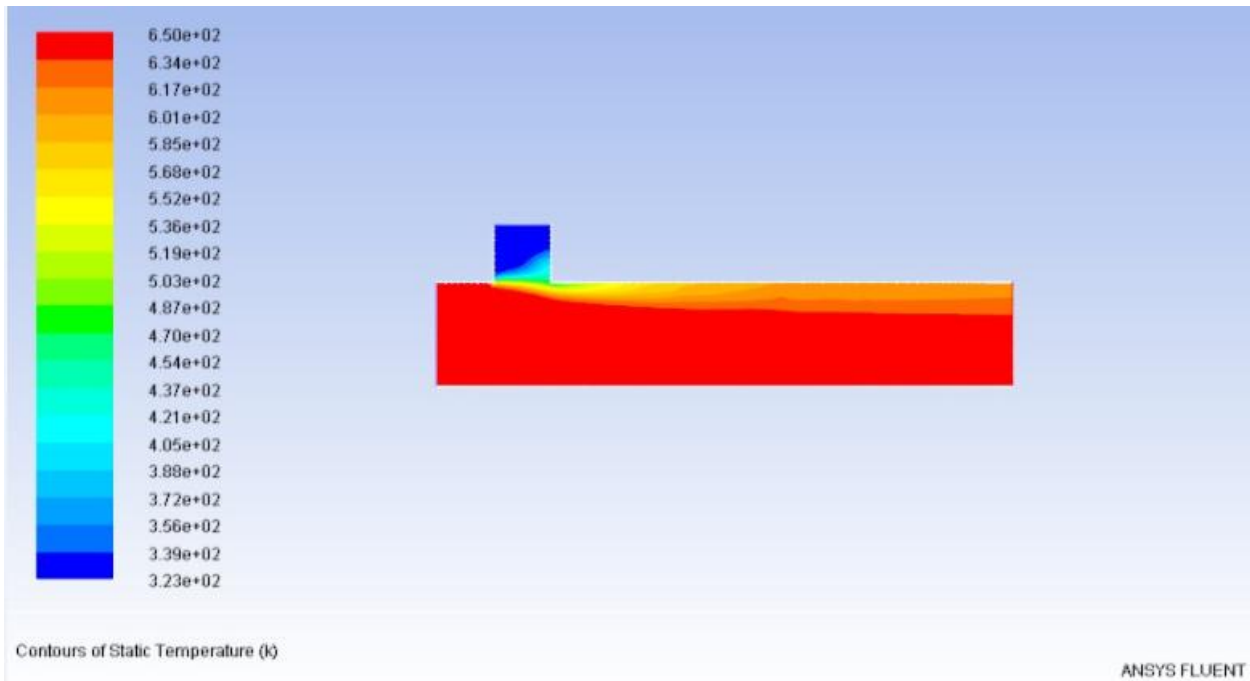


Figure 14 the biomass is introduced from upper inlet with low velocity of 0.3m/s, whereas the supercritical water is introduced from left hand side with high velocity of 0.4 m/s.

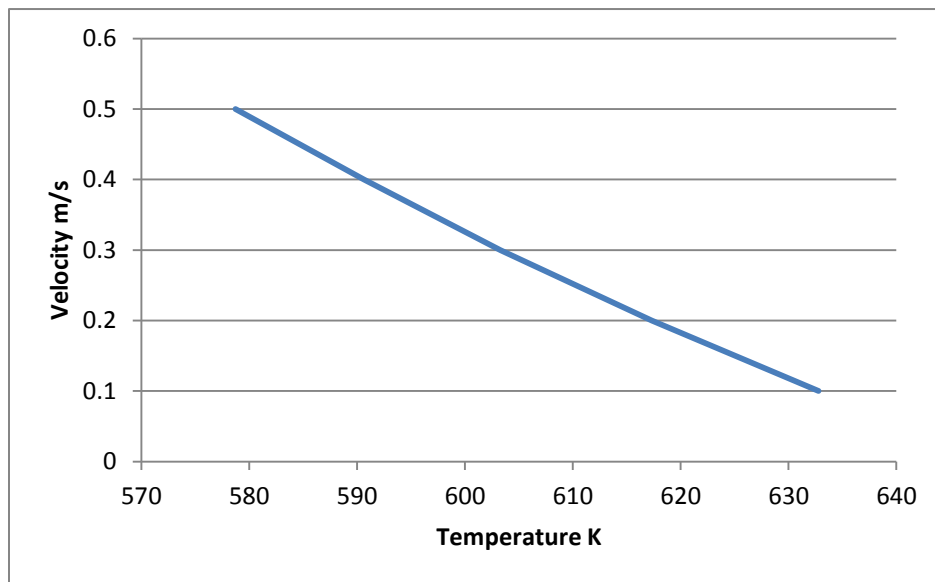
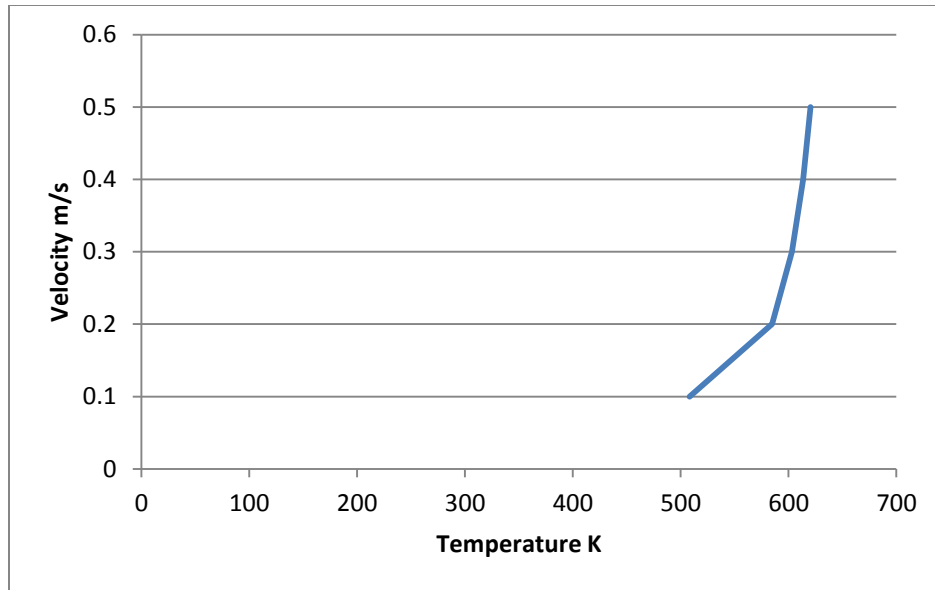


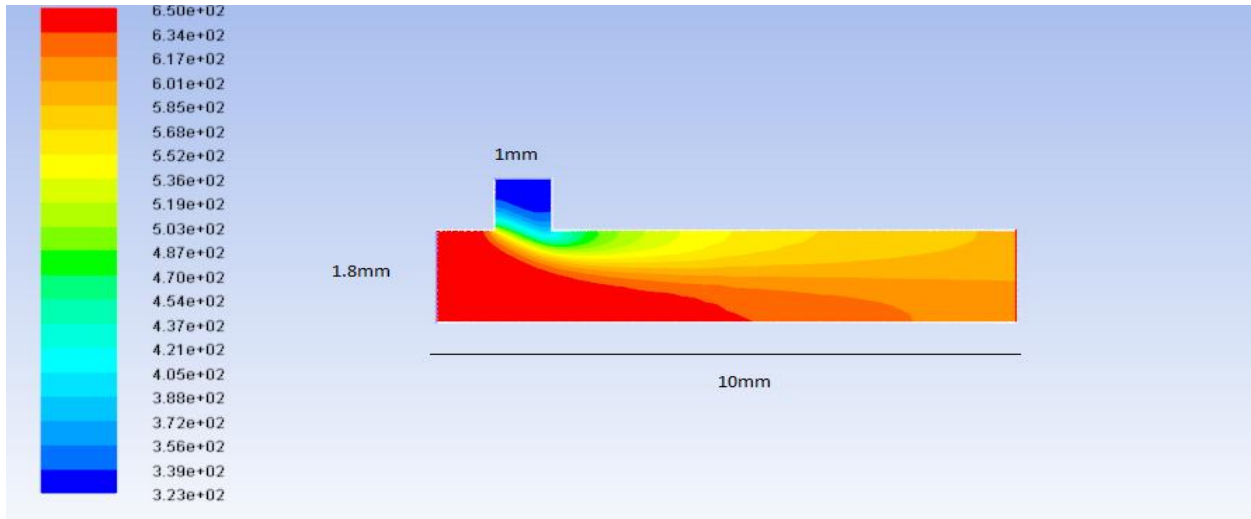
Figure 15 the velocity effect of biomass solution on outlet boundary at constant velocity of supercritical water.



**Figure 16 the velocity effect of supercritical water on outlet boundary at constant velocity of biomass solution.**

Figure 15 and 16, the fluid velocities have high dependency over outlet temperature. Therefore a good numbers of simulations have been run to find out the best velocities of the fluid at optimum temperature at outlet is achieved. These simulation results are compiled into graphical manner for better understanding. It is now obvious that increase in velocity of biomass solution, decreases the outlet temperature profile. If we chose highest velocity of biomass solution say 0.5m/s then temperature at outlet would be near to 570K, which is not desirable. On a contrary, the higher the velocity of super critical water, the higher the temperature gradient. Therefore we need to selected best combination of velocities that could achieve optimum temperature distribution at outlet.

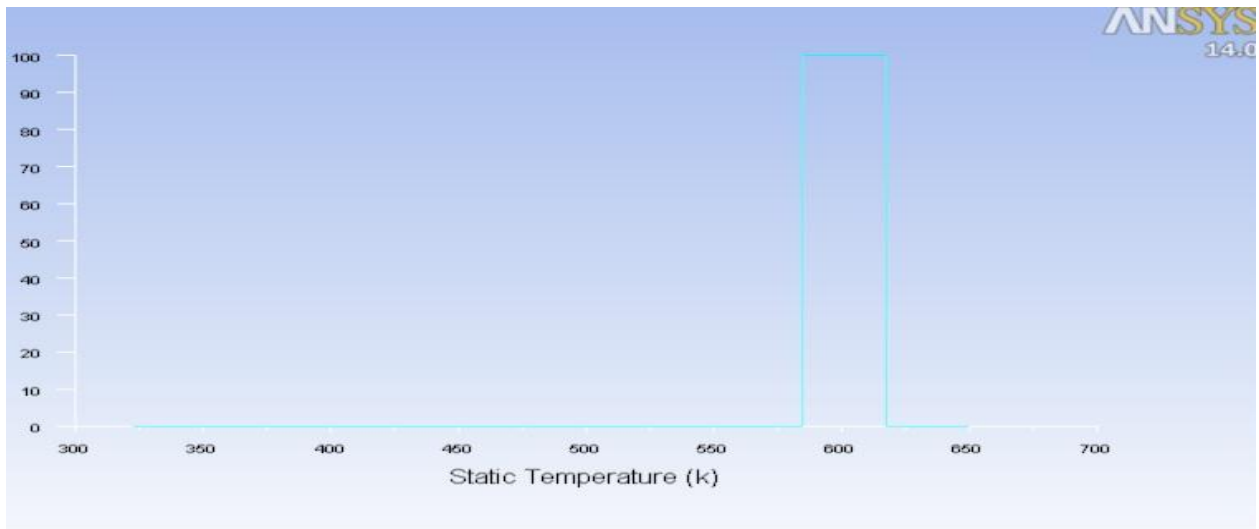
Figure 17, after checking all possible velocity combination, the optimum velocity of supercritical water is 0.3m/s and for biomass solution it is 0.1m/s. The average temperature at the outlet is 598K. The mass flow rate from inlet 1 and 2 is 6.6E-04 kg/s and 1.12 E-04 kg/s. At those velocities the biomass solution and supercritical water are well mixed inside the system. The most of biomass stayed at the center position that minimizes the accumulation of biomass particles on the wall. The temperature distribution inside the system is gradual and desirable. The temperature rise of substrate inside the reactor is 0.003 seconds which is similar to Yoshio work i.e. 0.001s. The temperature distribution at outlet is also showed by histogram in figure 18. The numerical values of histogram are attached in Appendix C.



Contours of Static Temperature (k)

ANSYS FLUENT 14.0

Figure 17 the biomass solution velocity is 0.1m/s and supercritical water is at 0.3m/s.



Jul 21, 2013  
ANSYS FLUENT 14.0 (2d, dp, pbns, ske)

Figure 18 Histogram profile of figure17 outlet surface, y-axis is the percentage of each temperature portion.

### 4.1.3 Effect of Velocity on Actual System

The actual geometry configuration is 6mm in diameter and 10mm in length. From previous task we got an idea about temperature dependency on fluid velocities, also the range of velocities for fluids. We start simulated different velocities for biomass solution and supercritical water, in order to achieve uniform distribution of temperature along with maximum mixing. Figure 19, if we decrease the velocity of biomass solution, the system showing non-mixed behavior with prominent hot spots. Figure 20, when the velocity of biomass solution is increased, the reactor temperature is divided into two parts .i.e. upper and lower. In upper part; which is blue colored, has the temperature of biomass only. Whereas in lower part; which is red colored, has prominent temperature of critical water only. We also notice slight mixing in the middle of the reactor; however that mixing portion is inadequate. Figure 21, lastly we tried to use same velocities for both biomass and critical water. The system shows adequate mixing in the upper part of the reactor but lower part is still dominated by the temperature of super critical water. From figure 19-21, it is obvious that the velocity which is developed in 4.1.2 could not be suitable for 6mm diameter. In all three cases, we observed hot spots and improper mixing. Therefore we need to try some other techniques to achieve optimum velocity for actual system i.e. 6mm diameter.

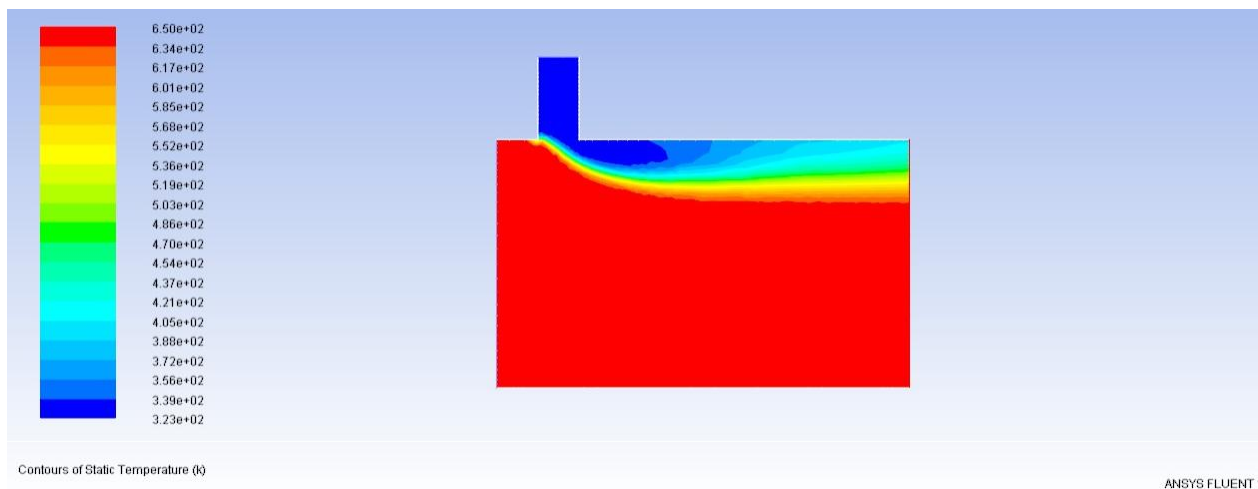


**Figure 19** the velocity of biomass solution is 0.2m/s whereas the velocity of supercritical water is 0.4m/s.

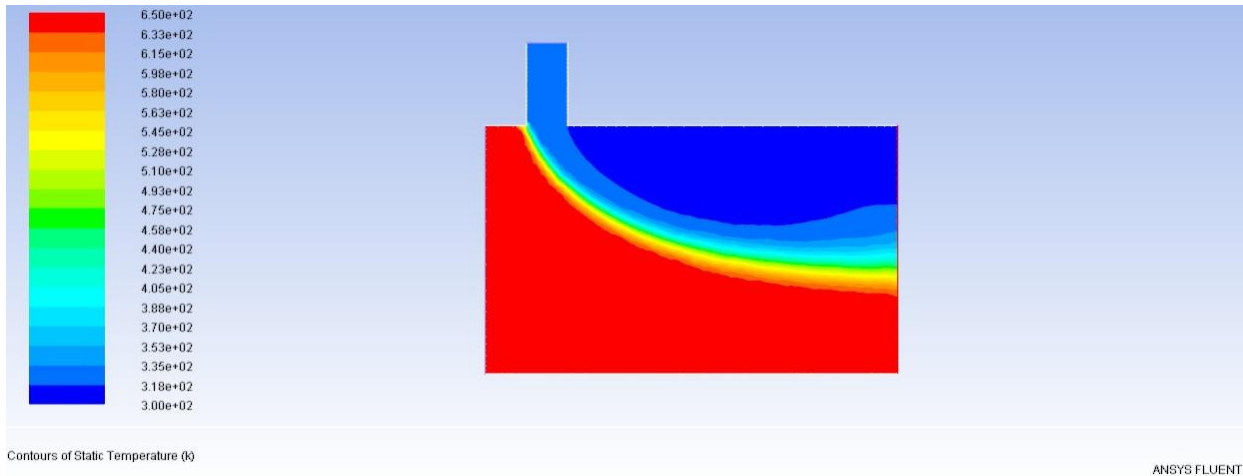


**Figure 20** the velocity of biomass solution is 0.4m/s whereas the velocity of supercritical water is 0.2m/s.

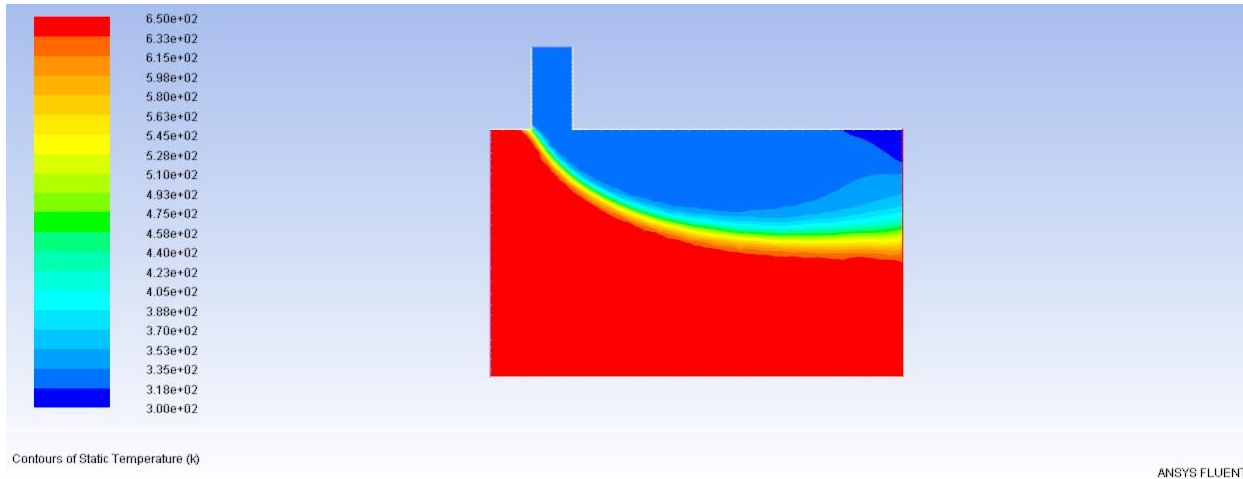


**Figure 21** the velocity of biomass solution and supercritical water is 0.3m/s each.

#### 4.1.4 Velocity Effect on Double Inlet for Super/Subcritical water

In figure 22, we introduced two inlets for supercritical water and one inlet for biomass. Furthermore, the biomass solution is introduced from left hand side, whereas the supercritical water is introduced from top and bottom inlets. The temperature of biomass solution and supercritical water remained same .i.e. 323K and 647K. The thermodynamic properties of water and the system remained same as discussed in ‘Method of Study’ section. Again we simulated different combination of velocities, we observed that the effect of double inlet for supercritical water is prominent and system is showing admissible results. The opted velocity for double inlets of supercritical water is 0.2m/s and for biomass solution it is 0.01m/s. It could be seen that



the critical water and biomass solution are well mixed; also the temperature distribution at the outlet is tremendous. The most of the biomass stay at the center of the reactor. The biomass particles are dispersing well at that velocity, and forming incremental increase in mixing.

In figure 23, histogram of figure 22 outlet surface is showed. According to histogram, the 90% of the temperature lies between 584.6K and 617.3K, whereas the 10% of the temperature is between 551.9-584.6K. The surface average temperature at outlet which is calculated by ANSYS fluent is 578K. The numerical values of histogram are mentioned in Appendix C.

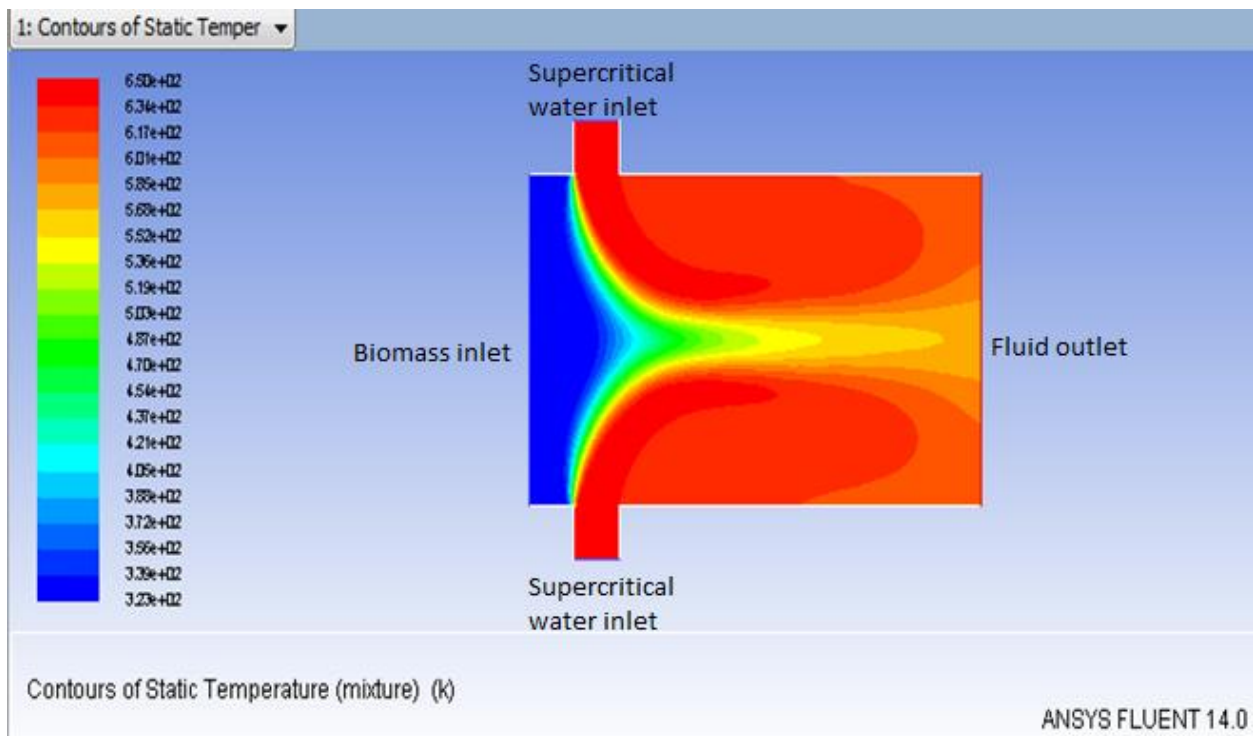


Figure 22 the velocity of biomass solution is 0.01m/s whereas the velocity of supercritical water is 0.2m/s each.

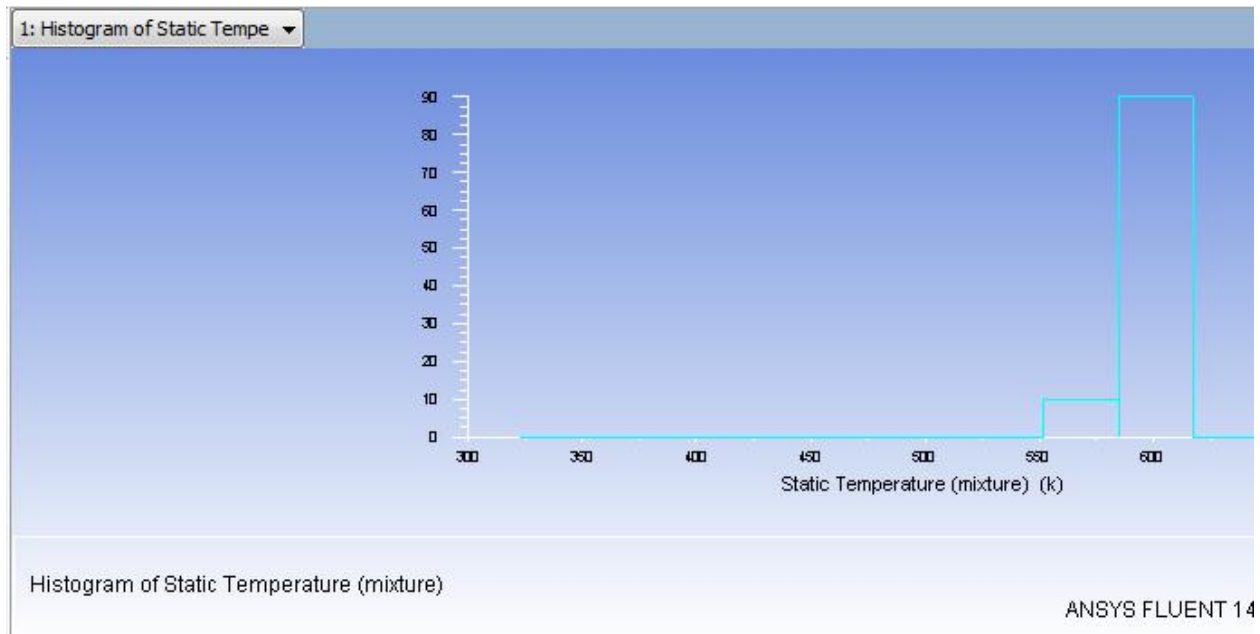


Figure 23 histogram of figure 22 outlet surface, y-axis is the percentage of each temperature portion.

#### 4.1.5 Effect of Inlet Diameter

In this task we study the behavior of inlets diameter on the system. The diameter of supercritical water is varied from 1-5mm. For each diameter range, the new geometry is been constructed in ANSYS gambit, the quality of geometry and mesh remained same as mentioned in table 3. The turbulent intensity as a function of diameter is calculated for each inlet diameter. We started simulated from 5mm diameter, at that diameter we had some convergence problem therefore we ignored the 5mm diameter of water. Later on we decreased the diameter step by step until 1mm. It is observed that the effect of the inlet diameter over outlet temperature is not dominating as we expected. We concluded that larger the opening, lower the mixing is achieved and temperature distribution at outlet temperature is dominated by supercritical water temperature. In a nut shell, the inlet diameter must be kept lower. The effect of inlet diameter is mentioned in the figure 24 below:

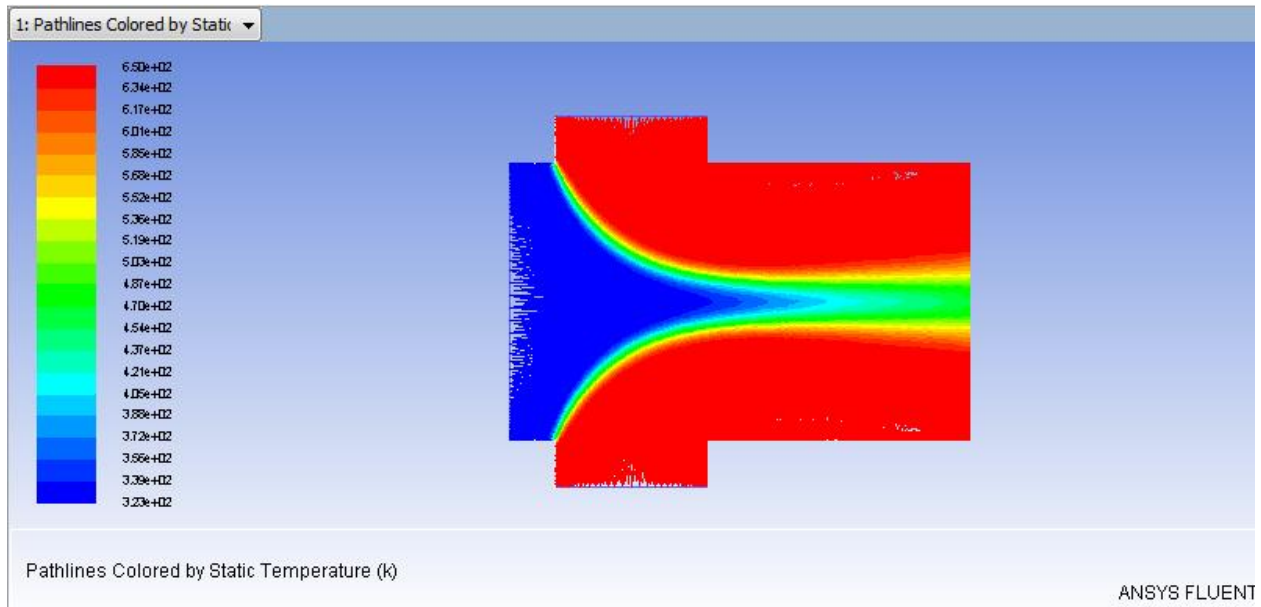


Figure 24 the effect of 3mm double inlet of supercritical water

## 4.2 Modeling for Reactor Containing Particles

### 4.2.1 Biomass Feed Effect

We study the effect of biomass feed percent inside the system, the biomass feed is varied from 5 to 10 % by weight. The velocity of biomass and subcritical water is 0.01m/s and 0.2 m/s. In task 4.1.4, we have already simulated it with 5% of biomass solution by weight. Therefore we started simulating from 10% of biomass; the solution takes a longer time to converge. The figure 25 shows that temperature distribution inside the system with 10% biomass. At that feed percentage of biomass, the uniform temperature is not achieved and fluid showing non-uniform mixing. The biomass tends to accumulate near boundary and there is a high possibility of choking; therefore it is not possible to use 10% feed concentration of biomass.

We repeated the simulation with lesser percentage of biomass. The behavior is almost similar from 3 to 6 % of biomass, however at 7% of biomass there is slight variation which is showed in figure 26. To conclude, the optimum feed percentage of biomass is achieved at 5-6%. If we further increase the feed percentage, we would get accumulation and choking. Also the temperature distribution could not be achieved uniform at the outlet.

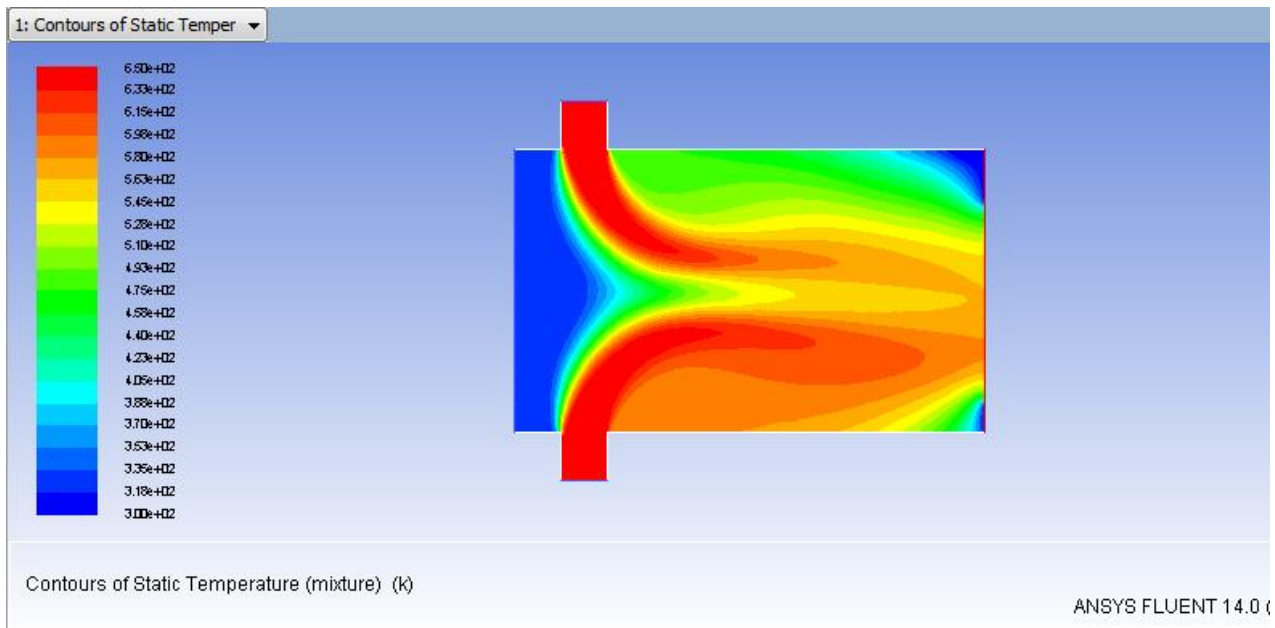


**Figure 25 temperature distribution inside the reactor with 10% biomass solution by weight**

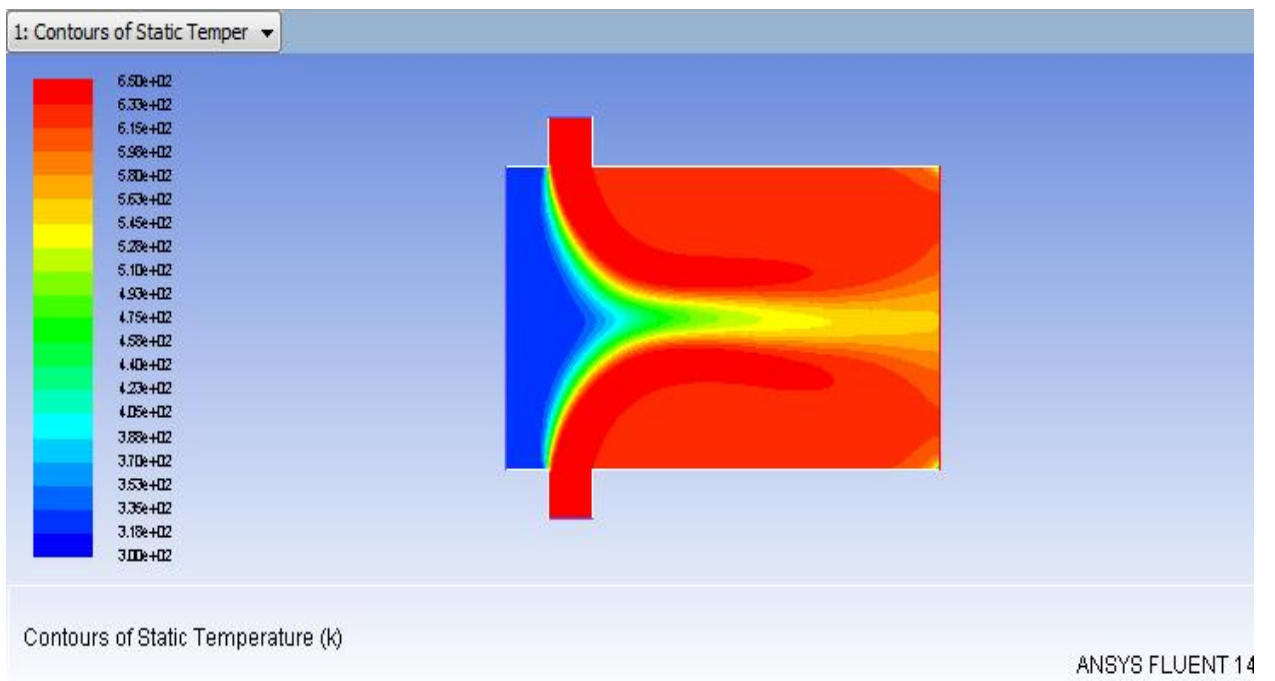


**Figure 26 temperature distribution inside the reactor with 7% biomass solution by weight.**

#### 4.2.2 Particle Movement inside the Reactor

Before studying particle movement inside the system, we investigated the relative velocity of biomass solution and supercritical water, which is showed in figure 27. According to figure 27, initially the velocity of biomass solution is low as it enters the system from left hand side. As the biomass get mix with the supercritical water the overall velocity of mixture has increased and reached to 0.21m/s at outlet. We observed slight variation in the velocity plot along the length of the reactor, that might be because of computational error or small or large eddies.

In order to be sure that our system contains no large/small eddies, we introduced weightless particles in the system. Particle movement is key element to understand the behavior of particle flow in a system. If the particle is entangled or rotates then there is high possibility to have unwanted side reactions. There is a chance of entanglement or rotation of particle due to inappropriate velocities of biomass solution and supercritical water. The possibility of small eddies might form between biomass and supercritical water inlets region due to low velocity, and the large eddies might occur before outlet as showed in velocity graph.

Figure 28: We introduce a single weightless particle from left hand side (biomass inlet) and place it at position (0,3). The interaction of weightless particle with continuous medium (critical water) is enabled. The particle tracking is also enabled in ANSYS fluent software. The relative velocity of the particle is 0.2m/s which is calculated by software. We kept default setting for number of iteration for disperse weightless particle. The movement of the particle is smooth inside the reactor from inlet of biomass solution to outlet, which indicate that the propose velocities of biomass solution and supercritical water is well set. The velocity does not create any small or large eddies.

The particle movement of our case is also validated with Yoshio Masuda work (Yoshio Masuda 2006). Figure 29: The Yoshio Masuda has used weightless particle to validate the movement of particle in T-Mixer, Yoshio introduced the weightless particle from right hand side of the mixer and observe the movement. The particle movement is smooth .i.e. no rotation which is similar with our case.

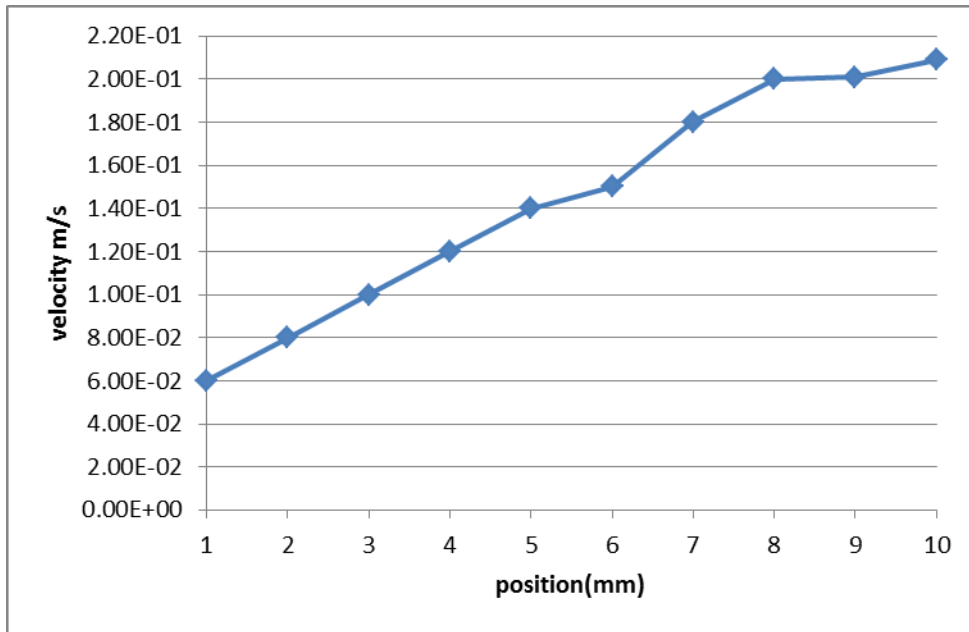


Figure 27 relative velocity of biomass solution and supercritical water along the length of reaction at position (0,3)

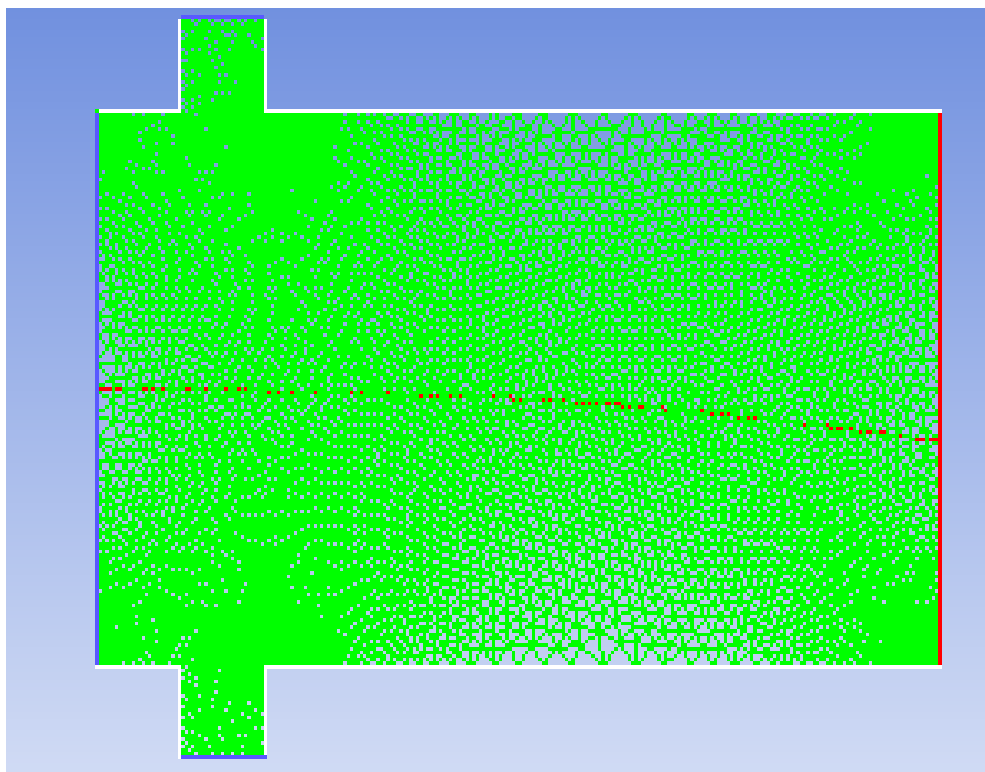


Figure 28 weightless particles is introduced from biomass inlet surface (0,3)position

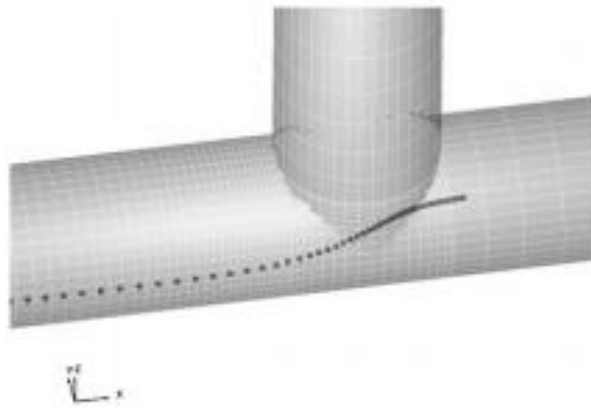


Figure 29 Yoshio Masuda introduced weightless particle from right hand side of the mixer.

### 4.3 Modeling of Reactions

#### 4.3.1 Density of Sub/Supercritical Water inside the Reactor

The decomposition reactions of biomass in sub and supercritical water are highly dependent over ionic products of water. If the density of water decreases with increase of temperature, the higher number of ionic products .i.e.  $H^+$  and  $OH^-$  are achieved; as a result of it the better decomposition reaction of biomass is expected. To validate this behavior of water, the density of water is defined as a function of temperature in ANSYS fluent by polynomial command.

In figure 30, the density of water changes and tends to decrease from inlet to outlet. This behavior of water is logical because at biomass inlet; the temperature of biomass solution is lower i.e. 323K. As the water proceed forward towards outlet the spontaneous rise of temperature decrease the density of water. At position 1mm of reactor the density of water is around  $900\text{kg/m}^3$  and at outlet position 10mm the density is turned out to be  $450\text{kg/m}^3$ .

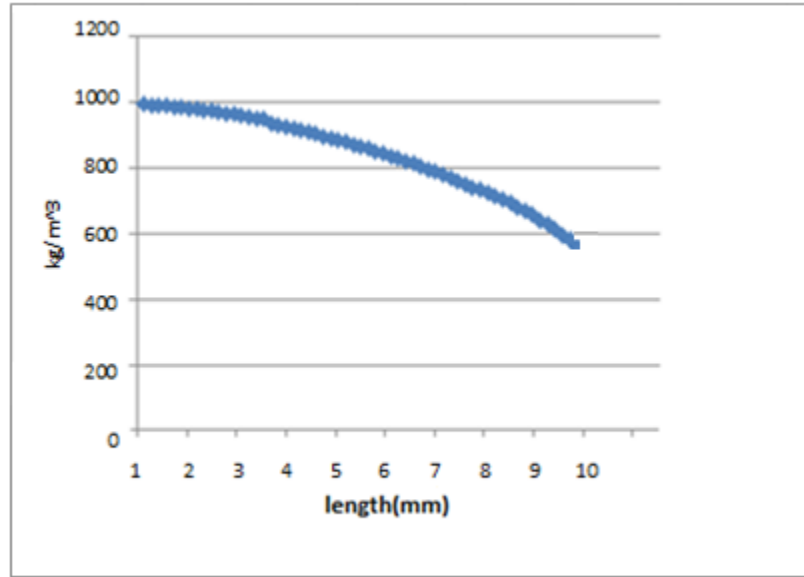


Figure 30 density of water along the length of reactor at position (0,3)

#### 4.3.2 Reactions by ANSYS Fluent

Initially the biomass reactions are conducted into ANSYS fluent software. The reactions type is volumetric finite-rate under species transport model. The Arrhenius parameters for cellulose decomposition to glucose are  $97.5E03$  J/k.mol activating energy and  $1E09$  pre-exponent factor. The stoichiometry coefficient and rate exponent for cellulose reaction is not defined in the paper; therefore we assumed it to be 1 for each. For lignin the activating energy is  $43.1E03$  and pre-exponent factor is  $10E03$ , we again assume stoichiometry coefficient and rate exponent be 1.

The simulation is conducted with 7000 iterations, which took around 40-50minutes. The solution could not be converged at the end of simulation as showed in figure 31. This behavior shows the error in stoichiometry and rate exponent values, these values are needed to be developed experimentally in near future. The non-authentic mass fraction of glucose and lignin decomposition is mentioned in the Appendix D.



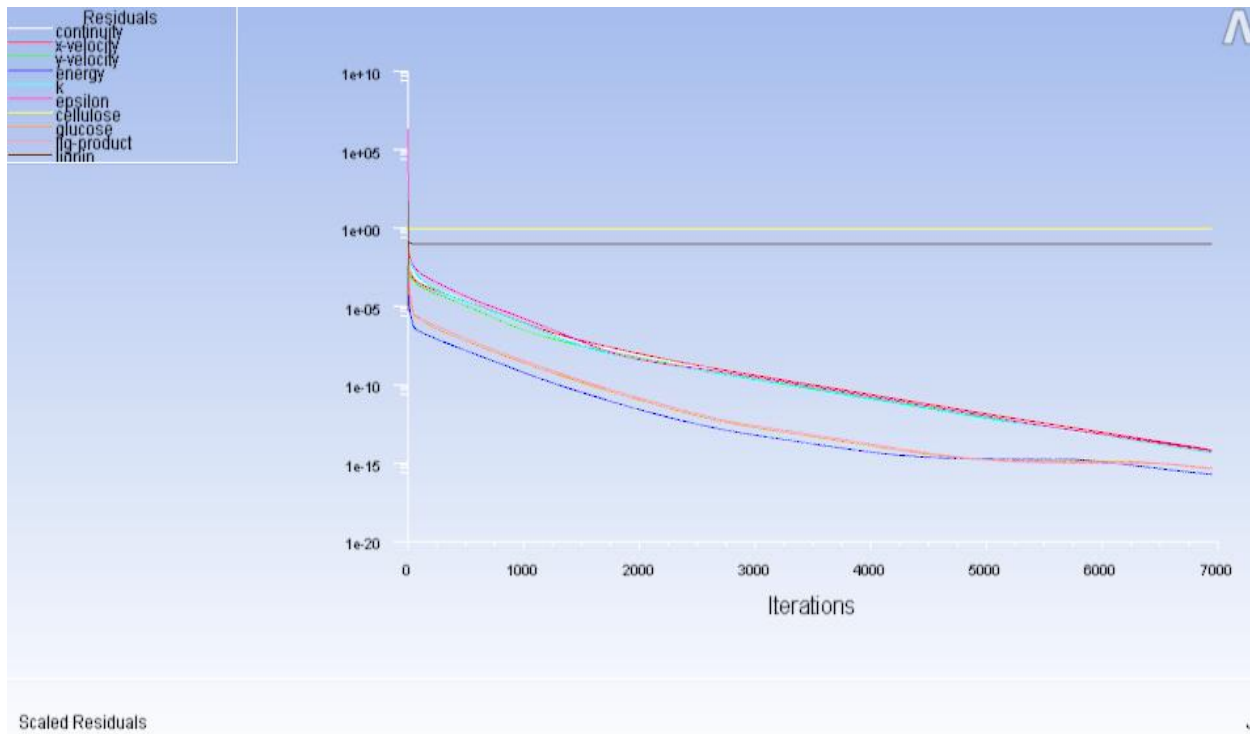


Figure 31 the non-converge residues(y-axis)of cellulose and lignin until the 7000 iterations.

### 4.3.3 Reactions by MATLAB

Since the authentic CFD simulation for reacting particles could not be performed, therefore we have used MATLAB software to predict the cellulose and lignin decomposition at 573K temperature. The Arrhenius equation (see 2.5) is solved in MATLAB and the code files along with function files are attached in Appendix E.

In figure 32, the decomposition of cellulose is mentioned as a function of time at 573K. The cellulose decomposes to glucose and then glucose to degraded-products. The calculated rate constant for cellulose decomposition into glucose is  $1.290 \text{ s}^{-1}$ . The adopted rate constant for glucose decomposition to by-product at 573K temperature is  $5.04 \text{ s}^{-1}$  (2.5.1). The cellulose conversion is 72% in 1 second time, which is greater than 69.8% in 0.78 second residence time (showed in red circle in table2). The decompositions of cellulose and glucose occur simultaneously because it is also observed that the decomposition of glucose to degraded-product is very fast too. At 1 second residence time, the production of degraded-product of glucose is around 61% and glucose concentration is 10%. As the residence time increases, the conversion of cellulose is increased too. At 3seconds the conversion of cellulose is expected to be 99%, which might be not true because according to Guang Yong Zhu in (2.5.1) that cellulose produces by-products. However, to validate that 99% conversion of cellulose we need to perform the experimental work, which will be done in near future.

In figure 33; the decomposition of lignin is elucidated at 573K temperature. The conversion of lignin in subcritical water as a function of time is simulated. Lignin follows number of parallel reaction and decomposes into three major products total organic components (TOC), gas and char. The conversion of lignin increases with increase in residence time. Lignin produces all three products .i.e. TOC, gas and char simultaneously because of the parallel reaction type. At 1second the conversion of lignin is 58.2% which seems to be reasonable as lignin is composed of complex interlinked branch structure. At that residence time the production of TOC is around 40%, whereas the produce char and gas are 15% and 3%. The maximum conversion of lignin could be achieved at residence time of 6seconds, which produces around 70% TOC, 25%char and 5% gas.

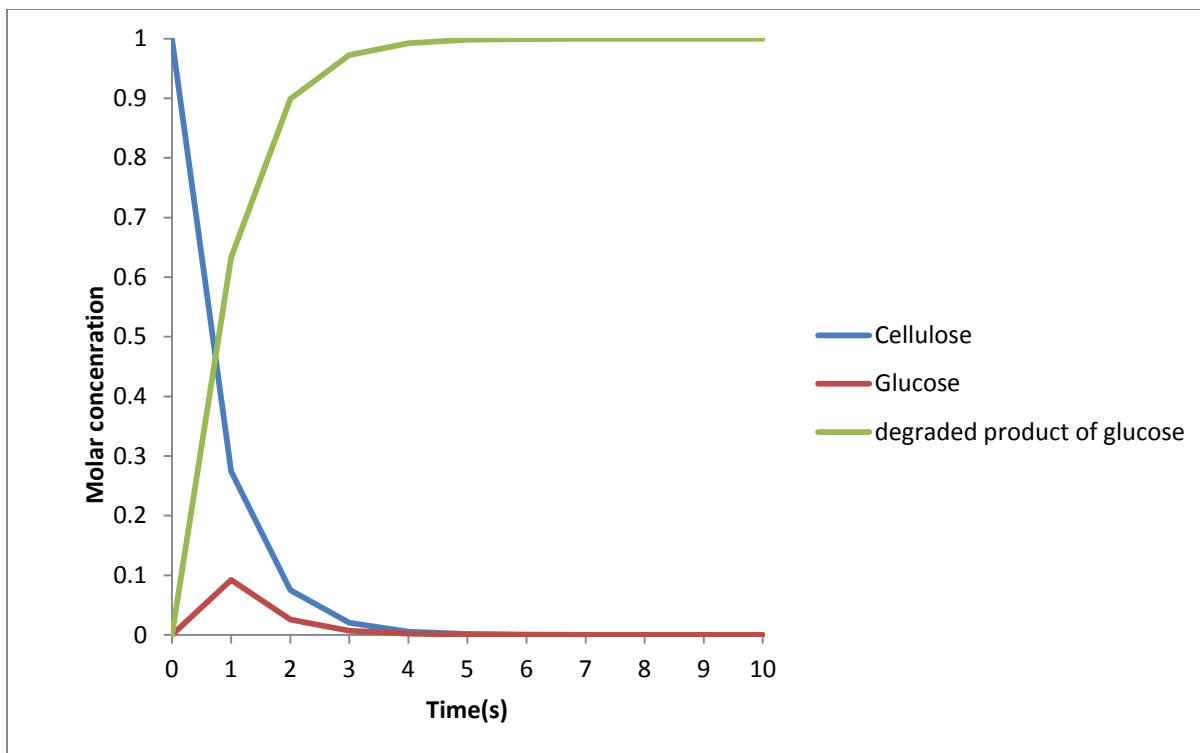


Figure 32 decomposition of species as a function of time.

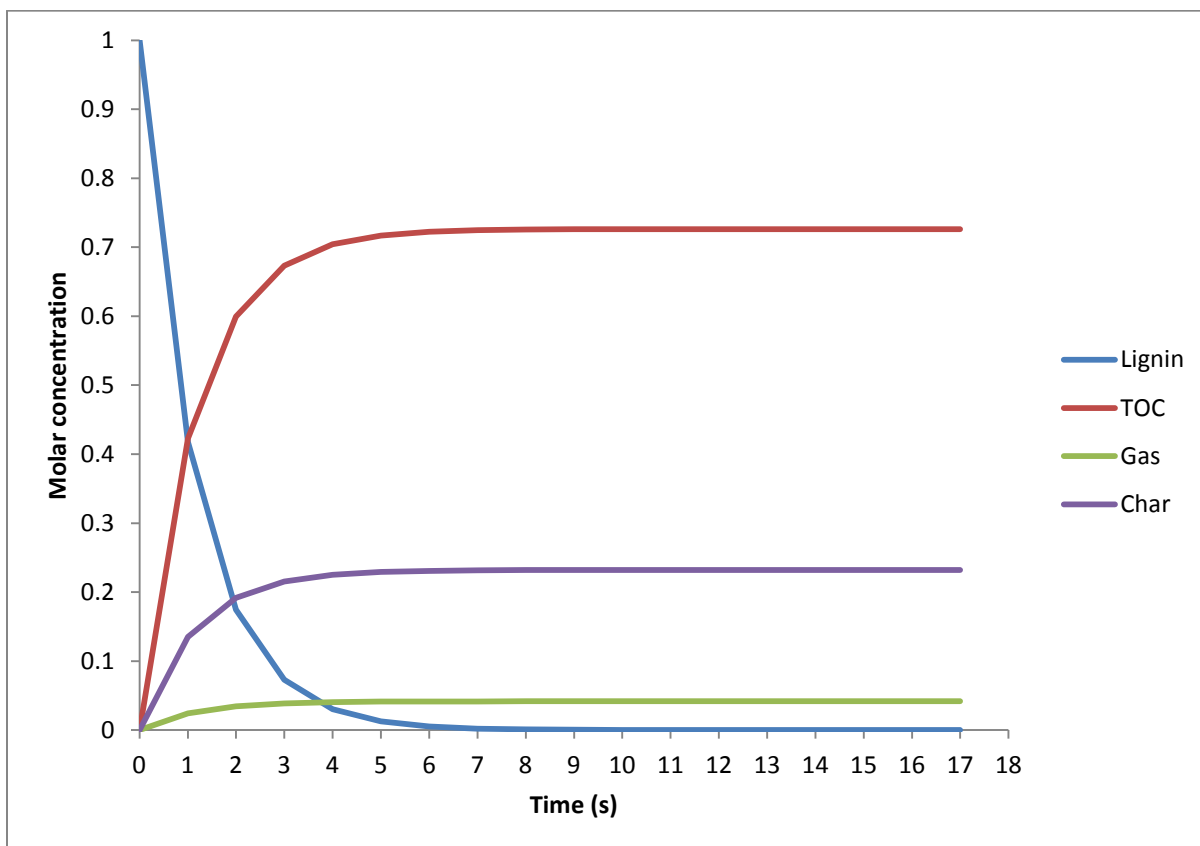


Figure 33 decomposition of lignin as a function of time.

#### 4.3.4 Effect of temperature on cellulose conversion

The effect of temperature on cellulose conversion is investigated to validate our system, when the temperature is changed. We know that the rate constant is a function of temperature; therefore the change in temperature will change the conversion rate. In figure 34, it is clearly observed that rate constant is well defined by Arrhenius parameters. As the temperature increase the conversion of cellulose is increased too i.e. directly proportional. In our system the average range of temperature is from 570K to 585K, therefore the expected conversion of cellulose is between 68-75%.

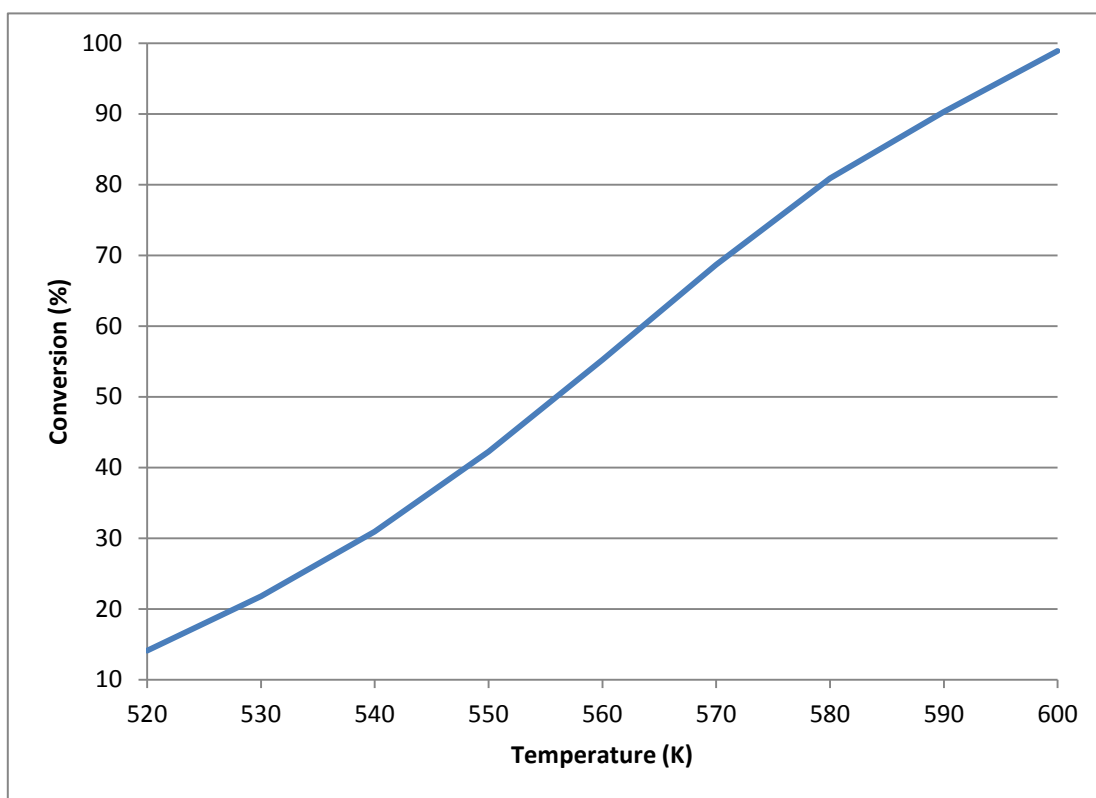
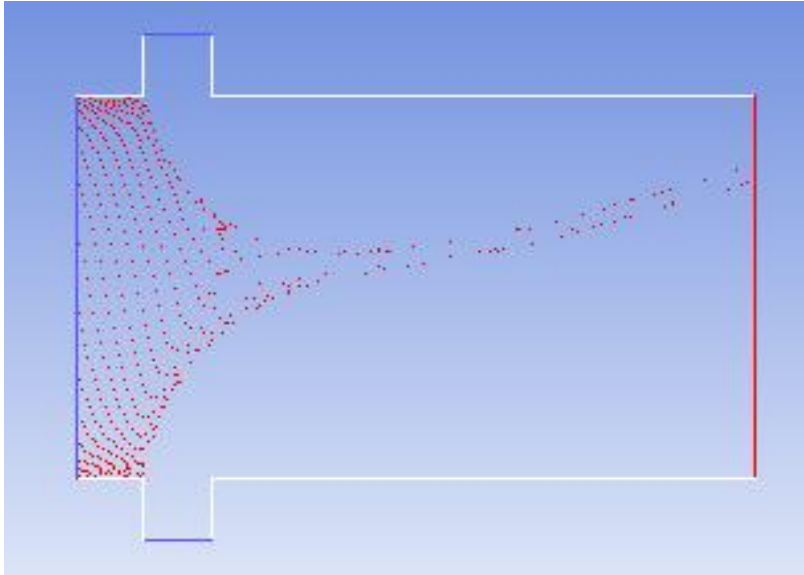


Figure 34 conversion of cellulose as a function of temperature.

#### 4.4 Modeling of Real Biomass Particle

In figure 35, the particle size is 10microns. Since the particle size is very small and particles at that size behave like weightless particle therefore the particles follow continuous medium i.e. critical water. The particle size is increased to 100microns which is demonstrated in figure36; there is small turbulence in the particle laden flow. The particle tends to make slight changes in the fluid flow due to larger diameter especially at the outlet boundary; where it could be observed that particles are scattering. In both cases the particles are accumulated in the middle of the reactor and forming a narrow curve. This narrow curve is not desirable because the particles are not fully exposed to subcritical water for reactions and making shorter contact time with subcritical water. Therefore both the results are not satisfactory, and further simulations are made.

After simulated different particle diameter (Appendix G), the opted diameter of particle is 500microns, which is showed in figure 37. At the biomass inlet (left hand side) the particles follow biomass velocity which is lower than supercritical water. As the particles proceed further, the velocity of the mixture increases. The increase in velocity makes the particle turbulent and creates disturbance in the system. This disturbance is highly desirable because it scatters the particles from each other inside the system. In this case we also observed that though the particles are in the center of the reactor, they are not making narrow curve as discuss above, hence providing enough space for the reaction with supercritical water. Furthermore only few particles are spreading near wall, which minimizes the accumulation problem inside the reactor. Figure 38 is simulated with 1000 microns; the particles are segregated inside the system. The most of the particles are found near wall due to the larger particle size, which might provoke choking and wall accumulation problem inside 6mm geometry. Therefore it is not admissible.



**Figure 35** red dots represent the diameter of particle, which is 10microns in this case.

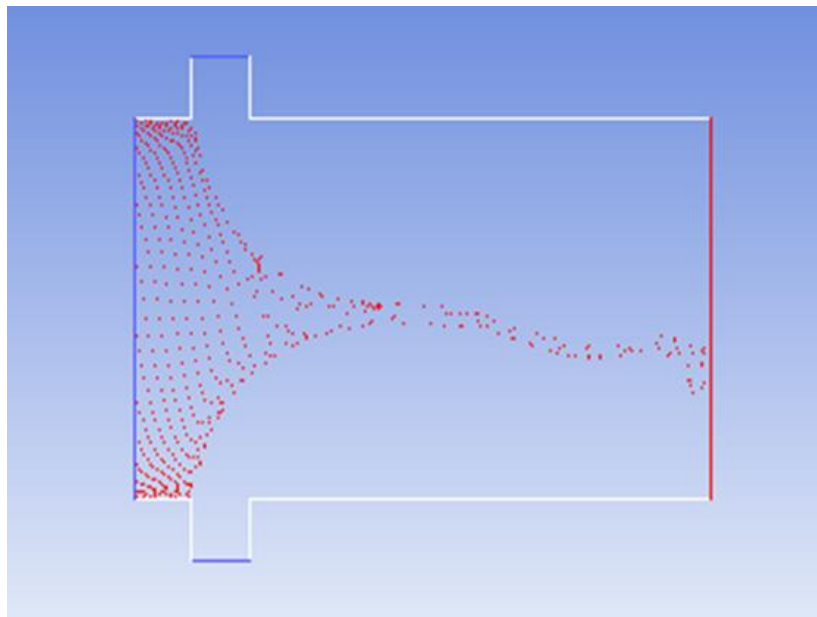


**Figure 36** red dots represent the diameter of particle, which is 100microns in this case.

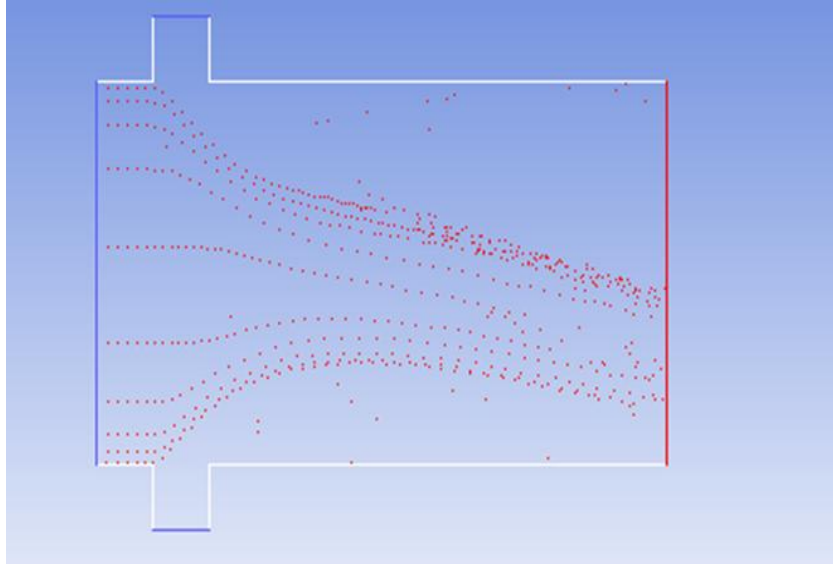


**Figure 37** red dots represent the diameter of particle, which is 500microns in this case.

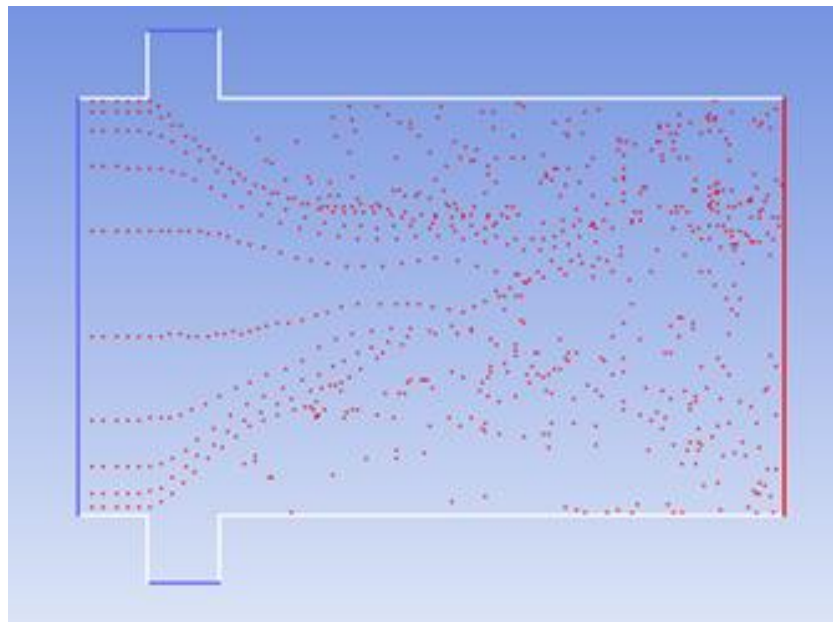


**Figure 38** red dots represent the diameter of particle, which is 1000microns in this case.

## 5 Conclusions

- The hydrothermal liquefaction of biomass in continuous flow tubular reactors is simulated using computational fluid dynamics software ANSYS fluent and ANSYS gambit.
- The model components for biomass are cellulose, hemi-cellulose and lignin. Micro-reactor is used for simulation work. The continuous media is subcritical water which works as catalyst and precede the reactions.
- The adopted kinetic parameter for cellulose decomposition to glucose is  $97.5E03$  activating energy and  $10E08$  pre-exponential constant. The rate constant for glucose decomposition into degraded-product is  $5.05s^{-1}$ . The rate constants for parallel decomposition reactions of lignin into TOC, gas and char are  $6.35E-01$ ,  $3.65E-02$  and  $2.03E-01$ .
- The mixture model is used for multiphase flow with energy equations and turbulence model (k-epsilon).
- The geometry is constructed on ANSYS gambit with different magnitudes, the opted dimension of the geometry is 10mm in length, 6mm in diameter and 1mm each diameter for upper and lower inlets. The aspect ratio is  $7.29E-1$  and orthogonal quality is 0.73.
- The temperature and velocity of the biomass solution is 323K and 0.01m/s, whereas the temperature and velocity for sub/supercritical water is 647K and 0.2m/s. The surface average temperature at the outlet is 578K
- The inlet diameter has no dominant effect on the fluid flow inside the system. The feed percent for biomass solution is 5% by weight. No formation of large/small eddies are found in the reactor.
- The biomass reactions in ANSYS fluent are not authentic because the solution is not converged.
- The biomass reactions in MATLAB are done by solving Arrhenius equation. The maximum conversion of cellulose in 1second is 72% at 573K temperature and produces 62% degraded-product and 10% glucose. For lignin, the achieve conversion in 1second is 58.2% and produces 40% TOC, 15%char and around 3% gas.
- The opted spherical particle diameter is 500 microns.



## 6 Future Works

- The implementation of this study should be applied to hydrothermal gasification process and then experimental work must be conducted to validate the reactor parameters.
- Further study and research are needed for biomass thermodynamic properties and exact reaction mechanism. Also more investigation is required for reaction path of biomass in critical water.
- The experimental work is needed for more detailed chemistry of biomass; especially for hemi-cellulose. The modification in Arrhenius parameters of hemi-cellulose have to be developed in near future.
- The higher order of scheme for instance QUICK need to be used in ANSYS fluent for more accurate results.

## 7 Reference

Abhijit Shrotri, A. T., and Jorge N Beltramini Pretreatment process for dissolving cellulose in water and single step catalytic hydrolysis-hydrogenation to produce sorbitol. Australia ARC Centre of Excellence for Functional Nanomaterials, University of Queensland And Department of Chemical Engineering, Monash Univesity, Clayton VIC 3168 Australia.

Allen, R. G. (1996). "Relating the Hazen-Williams and Darcy-Weisbach Friction Loss Equations For Pressurized Irrigation." American society of Agricultural Engineering **6**: 685-693.

Anil R. Oroskar, K. M. V. d. B., Suheil F. Abdo (2001). "Intensification in Microstructured Unit Operations Performance Comparison Between Mega and Micro Scale." Proceedings in IMRET 4th, Springer: 153-163.

B. Potic, S. R. A. K., M.Ye, M.A. van der Hoef, J.A.M. Kuipers,W.P.M. van Swaaij (2005). "Fluidizationwith hot compressedwater inmicro-reactors." Chemical Engineering Science(60): 5982-5990.

Bakker, A. (2002). "Applied Computational Fluid Dynamics.". Retrieved 18.06.201, from <http://www.bakker.org/dartmouth06/engs150/10-rans.pdf>.

Bansal P, H. M., Reaff MJ, Lee JH, Bommarius AS. (2010). "Multivariate statistical analysis of X-ray data from cellulose: a new method to determine degree of crystallinity and predict hydrolysis rates." Bioresource Technology **101**(12): 4461-4471.

Basu, P. (2010). Biomass Gasification and Pyrolysis: Practical Design and Theory. USA, Elsevier

Becker, P. J. (2013). "Hydrothermal liquefaction -- the most promising path to a sustainable bio-oil production." Retrieved 27.07.2013, from [http://www.eurekalert.org/pub\\_releases/2013-02/au-hl020613.php](http://www.eurekalert.org/pub_releases/2013-02/au-hl020613.php).

Bell, K. R. E. a. a. A. T. (2012). "The kinetics of Brønsted acid-catalyzed hydrolysis of hemicellulose dissolved in 1-ethyl-3-methylimidazolium chloride." Royal Society of Chemistry(RCS) Advances **2**: 10028-10036.

Blokhin, A. V., et al. (2011). "Thermodynamic Properties of Plant Biomass Components. Heat Capacity, Combustion Energy, and Gasification Equilibria of Cellulose." Journal of Chemical & Engineering Data **56**(9): 3523-3531.

Bridgwater, A. V. (2012). "Review of fast pyrolysis of biomass and product upgrading." Biomass and Bioenergy **38**: 68-94.

Cai Y Ma, T. M., Xue Z Wang,Chris J Tighe, Robert Gruar and Jawwad A Darr (2011). "CFD simulation of fluid flow and heat transfer in a counter-current reactor system under supercritical conditions." RSC publishing(2): 279-286.

Cai Y. Ma, X. Z. W., Chris J. Tighe and Jawwad A. Darr (2012). Modelling and Simulation of Counter-Current and Confined Jet React Continuous Hydrothermal Flow Synthesis of Nano-materials U.K, University of Leeds,UK: 874-879.

Cai Y. Maa, C. J. T., Robert I. Guarb, Tariq Mahmuda, Jawwad A. Darrb, Xue Z.Wanga. (2011). "Numerical modelling of hydrothermal fluid flow and heat transfer in a tubular heat exchanger under near critical conditions." The Journal of Supercritical Fluids **57**: 236-246.

CFD-Online. "Turbulence Intensity ". Retrieved 22.04, 2013, from [http://www.cfd-online.com/Wiki/Turbulence\\_intensity](http://www.cfd-online.com/Wiki/Turbulence_intensity).

D. Humbird, R. D., L. Tao, C. Kinchin, and a. A. A. D. Hsu (2011). Process Design and Economics for Biochemical Conversion of Lignocellulosic Biomass to Ethanol U.S.A, NREL U.S. Department of Energy, Efficiency & Renewable Energy, : 1-147.

D. Knez evic´, W. P. M. v. S., and S. R. A. Kersten (2009). "Hydrothermal Conversion of Biomass: I, Glucose Conversion in Hot Compressed Water." Ind. Eng. Chemical **48**: 4741-4743.

D.M. Hargreaves, N.G. Wright (2007). "On the use of the k-ε model in commercial CFD software to model the neutral atmospheric boundary layer." Journal of Wind Engineering and Industrial Aerodynamics **95**(5): 355-369.

Dinesh Mohan, C. U. P., Jr, and Philip H. Steele§ (2006). "Pyrolysis of Wood/Biomass for Bio-oil: A Critical Review." Energy and Fuels **20**: 848-889.

Dinesh Mohana, C. U. P. J., Philip H. Steele (2006). "Single, binary and multi-component adsorption of copper and cadmium from aqueous solutions on Kraft lignin—a biosorbent." Journal of Colloid and Interface Science **297**(2): 489-504.

DTI (2006). [NNFCC]National Non-Food Crops Center. Second generation transport biofuel, a mission to the Netherlands, Germany and Finland UK, REPORT OF A DTI GLOBAL WATCH MISSION 28-32.

Energy, U. S. D. o. (2013). Whole Algae Hydrothermal Liquefaction Technology Pathway USA, National Renewable Energy Laboratory and Pacific Northwest National Laboratory 1-10.

Frans Goudriaan, J. N., Ed van den Berg (2006). Conversion Of Biomass Residues To Transportation Fuels With The HTU Process. Netherlands HVC Group

Goring, D. A. I. The physical chemistry of lignin Montral, Canada, McGill University.

Guang Yong Zhu, Z. B. Y., Feng Ping Ma, Yan Hua Ji, Wen Qi (2011). "Kinetics of Glucose Production from Cellulose by Hydrolysis in Sub-Critical Water." Advanced Materials Research **347-353**: 2672-2678.

guide, A. f. m. f. u. s. (2010). "Mutiphase model, VOF MODEL." 1108-1170.

Hendry, D. (2012). Investigation of Supercritical Fluids for Use in Biomass Processing & Carbon Recycling Chemical Engineering, The University of Missouri-Columbia **Doctor of Philosophy**

J. Perez , J. M.-D., T. de la Rubia and J. Martinez (2002). "Biodegradation and biological treatments of cellulose, hemicellulose and lignin: an overview." Springer(5): 53-63.

Jaehoon Choe, Y. K., Yeongdae Kim, Hyun-Seob Song, Kwang Ho Song (2003). "Micromixer as a continuous flow reactor for the synthesis of a pharmaceutical intermediate." Korean Journal of Chemical Engineering, Springer link **20**(2): 268-272.

Kamimoto, M. (2006). The Significance of Liquid Fuel Production from Woody Biomass. J. Advanced Industrial Science and Technology(AIST). Japan: 1-10.

Koppejan, S. V. L. a. J. (2008). Biomass Combustion and Co-firing. UK and USA, Earthscan.

Lope Tabil, P. A. a. M. K. (2011). Biofuel's Engineering Process Technology, chapter 18, Biomass Feedstock Pre-Processing -PART1

Marrone, B. Y. a. P. (2012). Sub and Supercritical Water for the Production of Fuel and Green Chemicals from Biomass. Pacific West Biomass Conference, SAIC. San Francisco, California 1-11.

Masato Morimoto, S. S., Toshimasa Takanohashi (2012). "Effect of water properties on the degradative extraction of asphaltene using supercritical water." Journal of Supercritical Fluids **68**: 113-116.

Matlosz, E., Baselt(Eds.) (2001). "Micro-reactor Technology." Springer.

Matsumura, T. L.-K. Y. a. Y. (2012). "Reaction Kinetics of the Lignin Conversion in Supercritical Water." Industrial & Engineering Chemistry Reserach **51**: 11975-11988.

Matsumura, T. L.-K. Y. a. Y. (2013). "Kinetic Analysis of Lignin Hydrothermal Conversion in Sub and Supercritical Water." Industrial & Engineering Chemistry Reserach **52**: 5626-5639.

Mazza, C. P. a. G. (2010). "Kinetic Modeling of Hemicellulose Hydrolysis from Triticale Straw in a Pressurized Low Polarity Water Flow-Through Reactor." Industrial & Engineering Chemistry Reserach **49**: 6367-6637.

McKendry, P. (2002). "Energy production from biomass (part 1): overview of biomass." Bioresource Technology **83**(1): 37-46.

Mustafa Balat, M. B., Elif Kirtay, Havva Balat (2009). "Main routes for the thermo-conversion of biomass into fuels and chemicals. Part 1: Pyrolysis systems." Energy Conversion and Management **50**(12): 3157-3157.

N.L Panwara, R. K., V.V Tyagi (2012). "Thermo chemical conversion of biomass – Eco friendly energy routes." Renewable and Sustainable Energy Reviews, Science direct. **16**(4): 1801-1816.

Nussbaumer, T. (2003). "Combustion and Co-combustion of Biomass: Fundamentals, Technologies, and Primary Measures for Emission Reduction." Energy & Fuel **17**(6): 1510-1521.

Olanrewaju, K. B. (2012). Reaction kinetics of cellulose hydrolysis in subcritical and supercritical water. Chemical and Biochemical Engineering, University of Iowa. Phd

Peter Quaak, H. K., Hubert stassen (1999). Energy from Biomass:A review of combustion and gasification Technologies. U.S.A, The world bank . Washington DC.

Pooya Azadia, R. F., Clement Vuillardot (2011). "Estimation of heating time in tubular supercritical water reactors." Journal of Supercritical Fluids **55**: 1038-1045.

Prof. Dr. Peter H. Seeberger, F. W. Micro-reactor Technology. Chemfiles. USA. **5**: 1-6.

Prof. Dr. Uwe Riedel, P. D. N. D. (2011). CFD Simulation of Biomass Gasification Using Detailed Chemistry. Naturwissenschaftlich-Mathematischen Gesamtfakultät. Germany, Ruprecht-Karls-Universität at Heidelberg

**Masters.**

Q.Hu, T. (2002). Chemical Modification, Properties and Usage of lignin. New York: 94-96.

S, K. C. a. L. and (2011). "Equilibrium modeling for a downdraft for cotton stalks biomass in comparison with experimental data " Journal of Chemical Engineering and Materials Science **2**(4): 61-68.

S.Moussiere, C. J.-D., P. Guichaardon,O.Boutin,H.A Turc,A.rOUBAUD,B.Fournel (2007). "Modelling of heat transfer and hydrodynamic with two kinetics approaches during supercritical water oxidation process." The Journal of Supercritical Fluids **43**: 324-332.

Scheraga, G. N. a. H. A. (1962). "Structure of Water and Hydrophobic Bonding in Proteins. I. A Model for the Thermodynamic Properties of Liquid Water8." The Journal of Chemical Physics **36**(12): 1-19.

Silvia Vivarelli, G. T. (2004). Pyrolysis Oil: An Innovative Liquid Biofuel for Heating. Italy, Bioenergy for a sustainable development.

Simon Dreher, N. K. a. P. W. (2009). "Characterization of Laminar, Transient flow regimes and Mixing in T-shaped Micromixers." Taylor & Francis **30**(1-2): 91-100.

Singhb, P. S. N. a. A. (2011). "Production of liquid biofuels from renewable resources." Progress in Energy and Combustion Science **37**(1): 52-68.

Sunkyu Park, J. O. B., Michael E Himmel, Philip A Parilla and David K Johnson<sup>1</sup> (2010). "Cellulose crystallinity index: measurement techniques and their impact on interpreting cellulase performance." Biotechnology and Biofuel **3**: 1-8.

Takafumi Aizawa, Y. M., Kimitaka Minami,Mitsuhiro Kanakubo,Hiroshi Nanjo,Richard L.Smith (2007). "Direct observation of channel-tee mixing of high temperature and high pressure water." Journal of Supercritical Fluids **43**: 222-227.

Taylor, R. S. a. M. (2008). From 1st to 2nd generation Biofuel Technologies France, International Energy Agency: 1-124.

Tom Bruton, D. H. L., Dr Yannick Lerat, Dr Michele Stanley, Michael Bo Rasmussen. (2009). A Review of the Potential of Marine Algae as a Source of Biofuel in Ireland Ireland, Sustainable Energy Ireland.

Valery B. Agbor , N. C., Richard Sparling , Alex Berlin, David B. Levin (2011). "Biomass pretreatment: Fundamentals toward application." Biotechnology Advances **29**.

Wyman, S. E. J. a. C. E. (2000). "Cellulose and Hemicellulose Hydrolysis Models for Application to Current and Novel Pretreatment Processes." Appl Biochem Biotechnol: 84-86.

Yan, Y. W. a. L. (2008). "CFD Studies on Biomass Thermochemical Conversion " international journal of molecular sciences(9): 1108-1130.

Yokoyama, S. (2008). Thermochemical conversion of biomass. The Asian Biomass Handbook, The Japan Institute of Energy. Japan: 94-114.

Yokoyama, T. O. a. S.-y. (1993). "Liquid Fuel Production from Woody Biomass By Direct Liquefaction." National Institute for Resources and Environment **36**(2): 73-84.

Yoshio Masuda, A. S., Yutaka Ikushima (2006). "Calculation method of heat and fluid flow in a microreactor for supercritical water and its solution." Heat and Mass Transfer **33**: 419-425.

Yun Yu, X. L., and Hongwei Wu (2008). "Some Recent Advances in Hydrolysis of Biomass in Hot-Compressed Water and Its Comparisons with Other Hydrolysis Methods†." Energy and Fuels **22**: 46-60.

Zhang, B., et al. (2008). "Reaction kinetics of the hydrothermal treatment of lignin." Appl Biochem Biotechnol **147**(1-3): 119-131.

Zhang, B., et al. (2012). "A Kinetics Study on Hydrothermal Liquefaction of High-diversity Grassland Perennials." Energy Sources, Part A: Recovery, Utilization, and Environmental Effects **34**(18): 1676-1687.

Zhang, B., et al. (2008). "Thermal effects on hydrothermal biomass liquefaction." Appl Biochem Biotechnol **147**(1-3): 143-150.

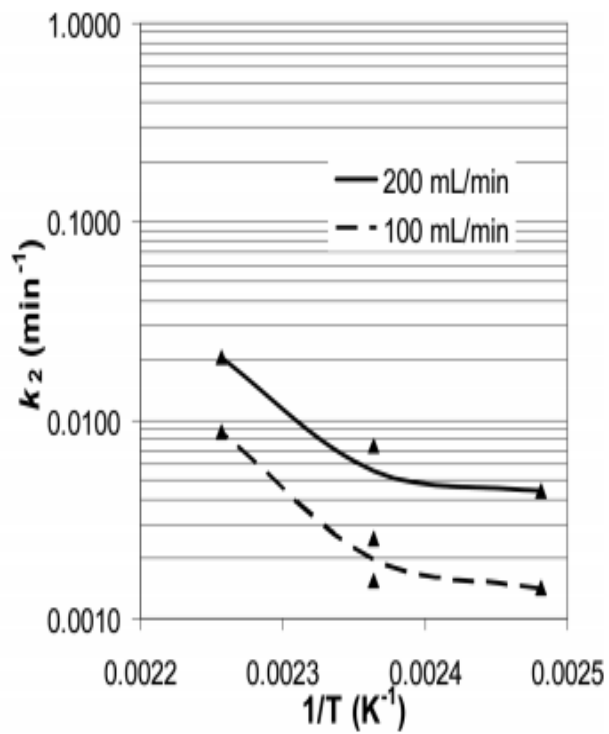
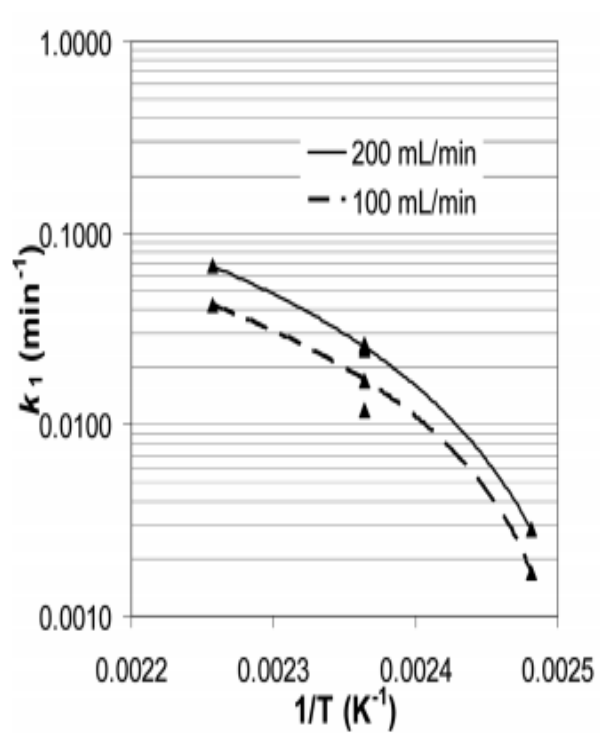
Zhang, T. (2008). Glucose production from Cellulose in Subcritical and supercritical water. Department of Chemical and Biochemical Engineering. USA, The University of Iowa. **PHD**.

Zhang, X., et al. (2011). "Routes to Potential Bioproducts from Lignocellulosic Biomass Lignin and Hemicelluloses." BioEnergy Research **4**(4): 246-257.

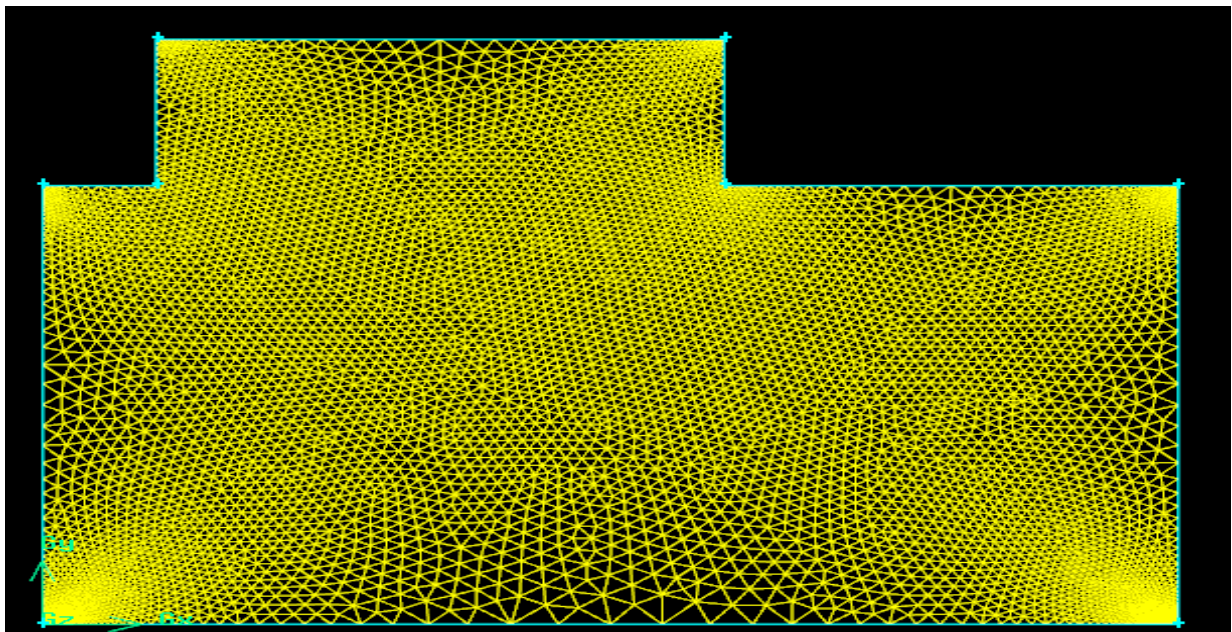
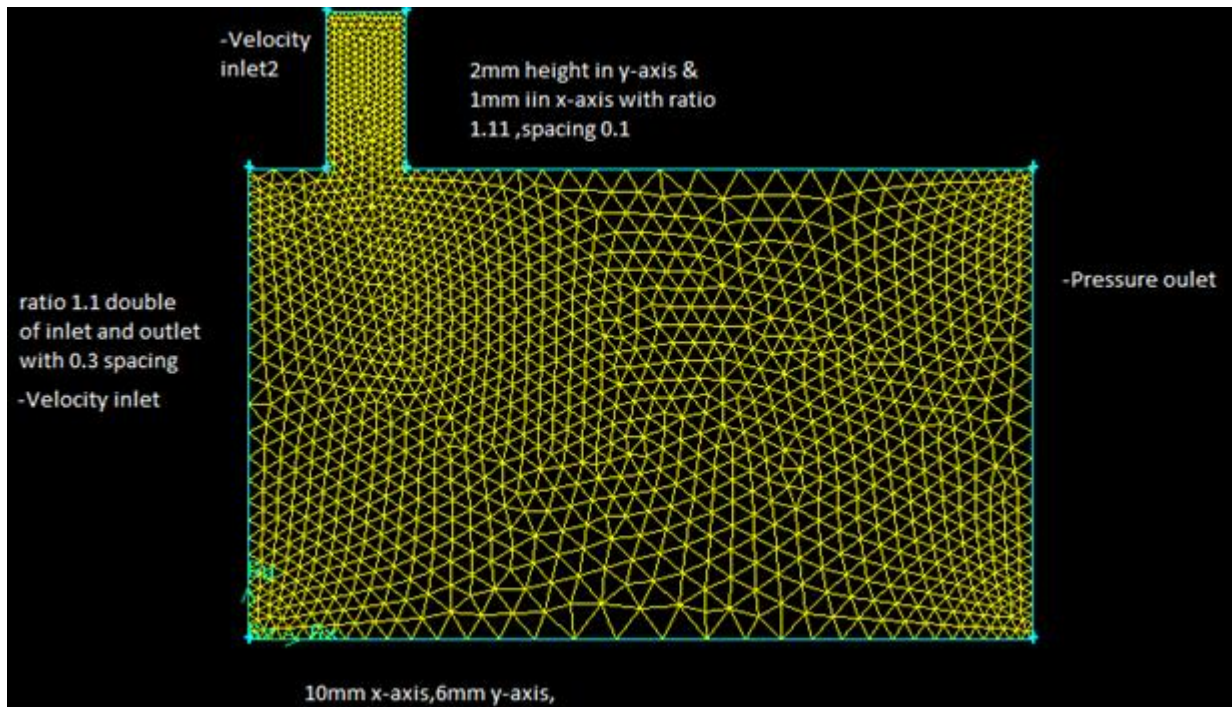
Zhang, Y. (2010). "Hydrothermal Liquefaction to Convert Biomass to Crude oil." Biofuel from Agricultural Wastes and Byproducts: 201-232.

Zhong, C. and X. Wei (2004). "A comparative experimental study on the liquefaction of wood." Energy **29**(11): 1731-1741.

## Appendix A: Non-Linear Arrhenius Parameter for Hemi-cellulose



## Appendix B: Geometry of difference dimensions





## Appendix C: Histogram values

### First Histogram:

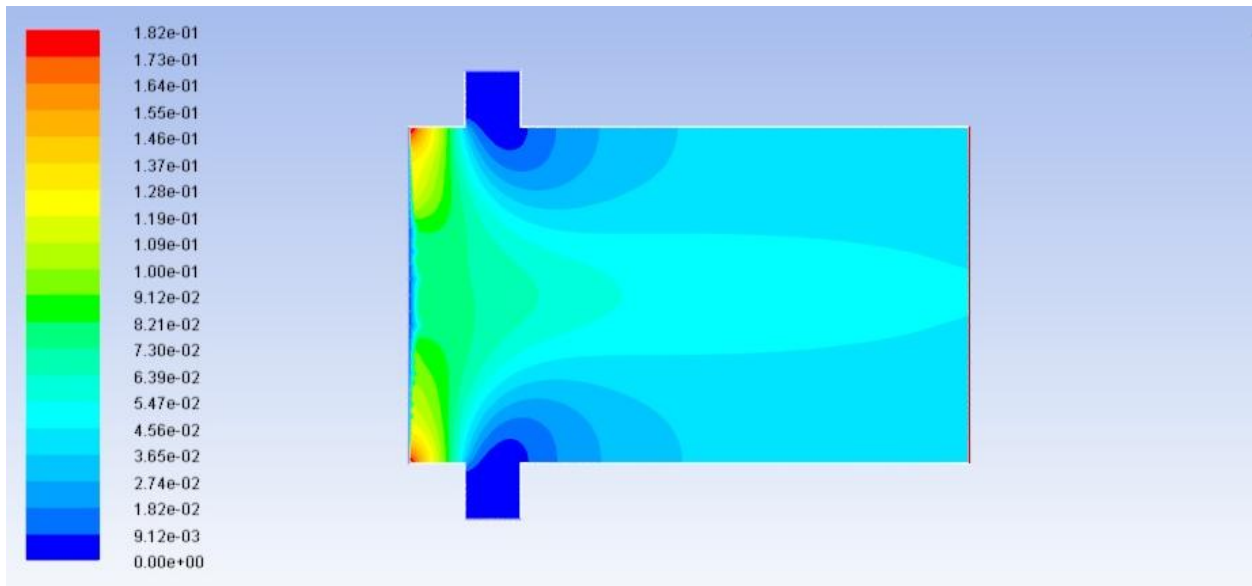
0 elements below 323 (0 %)  
0 elements between 323 and 355.70009 (0 %)  
0 elements between 355.70009 and 388.40018 (0 %)  
0 elements between 388.40018 and 421.10027 (0 %)  
0 elements between 421.10027 and 453.80037 (0 %)  
0 elements between 453.80037 and 486.50046 (0 %)  
0 elements between 486.50046 and 519.20055 (0 %)  
0 elements between 519.20055 and 551.90064 (0 %)  
0 elements between 551.90064 and 584.60073 (0 %)  
18 elements between 584.60073 and 617.30082 (100 %)  
0 elements between 617.30082 and 650.00092 (0 %)  
0 elements above 650.00092 (0 %)

**AND**

### Second Histogram:

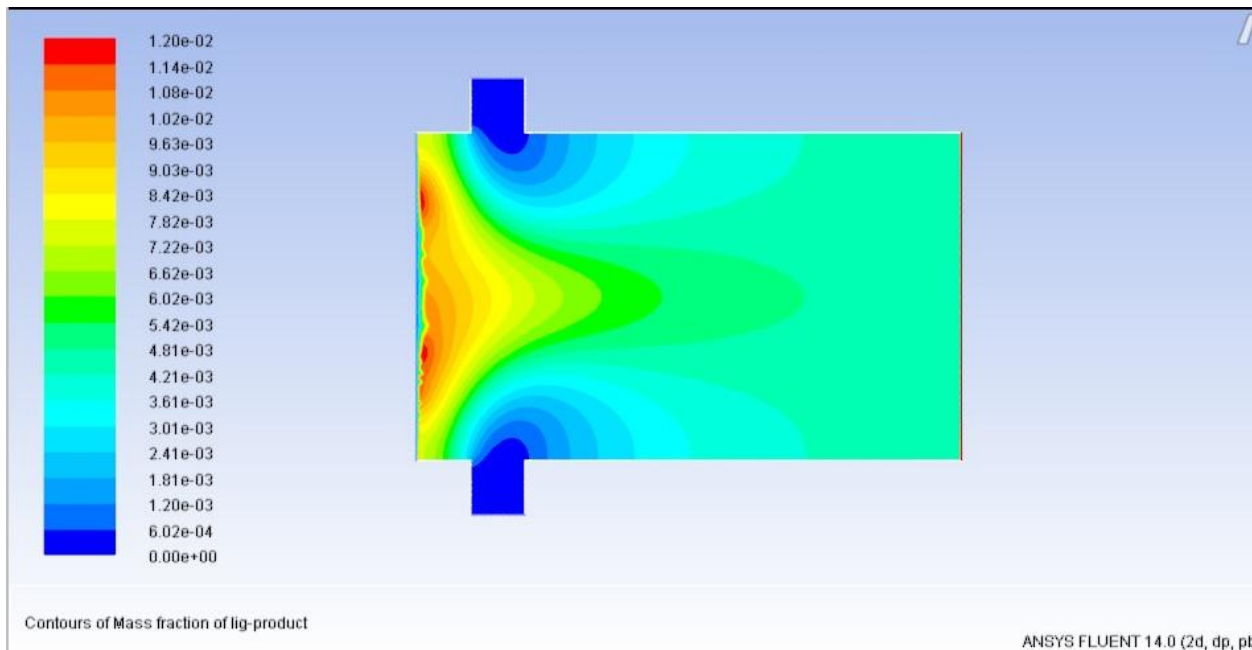
0 elements below 322.99982 (0 %)  
0 elements between 322.99982 and 355.70031 (0 %)  
0 elements between 355.70031 and 388.40081 (0 %)  
0 elements between 388.40081 and 421.1013 (0 %)  
0 elements between 421.1013 and 453.80179 (0 %)  
0 elements between 453.80179 and 486.50229 (0 %)  
0 elements between 486.50229 and 519.20278 (0 %)  
0 elements between 519.20278 and 551.90328 (0 %)  
6 elements between 551.90328 and 584.60377 (10 %)  
54 elements between 584.60377 and 617.30427 (90 %)  
0 elements between 617.30427 and 650.00476 (0 %)  
0 elements above 650.00476 (0 %)

## Appendix D: Contour of glucose and lignin-product mass fractions



Contours of Mass fraction of glucose

ANSYS FLUENT 14.0 (2d, dp)



Contours of Mass fraction of lig-product

ANSYS FLUENT 14.0 (2d, dp, pt)

## Appendix E: MATLAB files

```
modeling of cellulose and Ligin in continuos
%flow type reactor with short residence time in seconds
%first order irreversible reaction
%lowa thesis cellulose to glucose @ 573k, irreversible and 1st order reaction
clear all;clc;
s0=[1 0 0]; %initial concentration of Glucose & fructose
k0=[10e8 97.5e3 5.04];
% k0=[10e8 97.5e3 4.37e11 120e3];
ts=[0:1:10]; % linspace(0,100);
% ts=[0.005]
[t,s]=ode15s(@cellu_ode,ts,s0,[],k0);
plot(t,s);
X=(1-s(2,1))/1 %conversion

subplot(321)
plot(t,s(:,1));
xlabel('Time in seconds');
ylabel('molar concentration');
legend('cellulose');

subplot(322)
plot(t,s(:,2));
xlabel('Time in seconds');
ylabel('molar concentration');
legend('Glucose');

subplot(323)
plot(t,s(:,3));
xlabel('Time in seconds');
ylabel('molar concentration');
legend('Glucose-Prod:');

subplot(324)
plot(t,s);
xlabel('Time in seconds');
ylabel('molar concentration');
legend('Cellulose','Glucose','Glucose-Prod');

%% lignin (lignin to toc,gas and char @ temp 573k

clear all;clc;
s0=[1 0 0 0];
k0=[6.35e-1 3.65e-2 2.03e-1]; %toc, gas,char
ts=[0:1:17]; % linspace(0,100);
[t,s]=ode15s(@lignin_ode,ts,s0,[],k0);
X=(1-s(2,1))/1
subplot(321)
plot(t,s(:,1));
xlabel('Time in seconds');
ylabel('molar concentration');
legend('lignin');

subplot(322)
```

```

plot(t,s(:,2));
xlabel('Time in seconds');
ylabel('molar concentration');
legend('TOC');

subplot(323)
plot(t,s(:,3));
xlabel('Time in seconds');
ylabel('molar concentration');
legend('Gas');

subplot(324)
plot(t,s(:,4));
xlabel('Time in seconds');
ylabel('molar concentration');
legend('Char');

subplot(325)
plot(t,s);
xlabel('Time in seconds');
ylabel('molar concentration');
legend('Lignin','TOC','Gas','Char');
%%
%Hemi cellulose to xylone, irreversible and 1st order reaction
%series reaction
%H?k1*O ?k2*X ?k3*D
%H=hemi-cellulose,O=xylose-oligomers,X=xylose,D=degraded products
clear all;clc;
% s0=[1 0 0 0]; %initial concentration of Glucose &
fructose
s0=[1 0];
% k0=[10^9 99e3];
ts=[0:1:10]; % linspace(0,100);
[t,s]=ode15s(@hemi_ode,ts,s0,[]);
plot(t,s);
X=(1-s(2,1))/1

subplot(221)
plot(t,s(:,1));
xlabel('Time in seconds');
ylabel('molar concentration');
legend('Hemi-cellulose');

subplot(222)
plot(t,s(:,2));
xlabel('Time in seconds');
ylabel('molar concentration');
legend('Xylo-oligomers');

subplot(223)
plot(t,s);
xlabel('Time in seconds');
ylabel('molar concentration');
legend('Hemi-cellulose','Xylo-oligomers');

```

## Function files

```
function ds=cellu_ode(t,s,teta);
A=s(1);
B=s(2);
T=575;
R=8.314;
Aa=teta(1);E=teta(2);
k=Aa*exp(-E/R*1/T) ; %(1/T-1/Tmean));
% k1=teta(3)*exp(-teta(4)/R*1/T) ;
d=[-k*A
    k*A-teta(3)*B
    teta(3)*B];

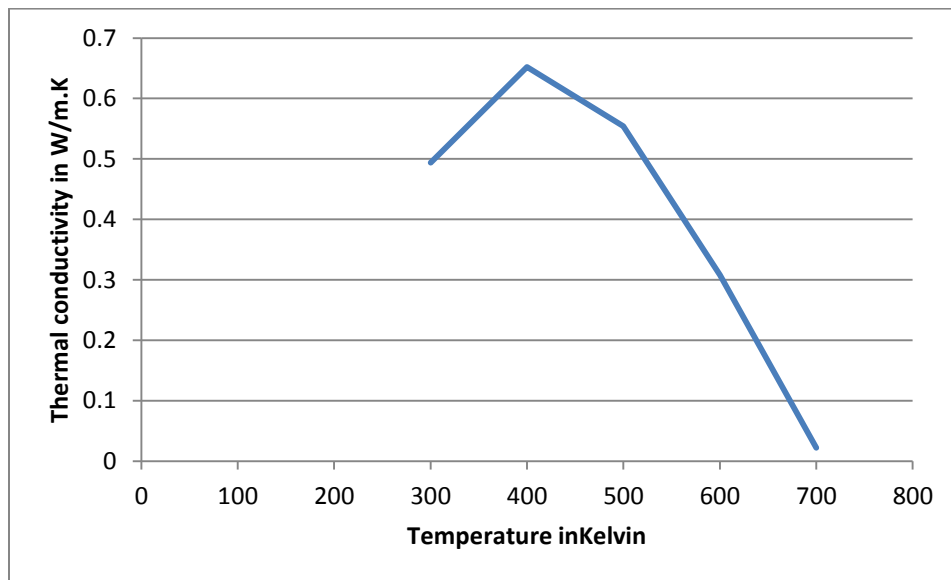
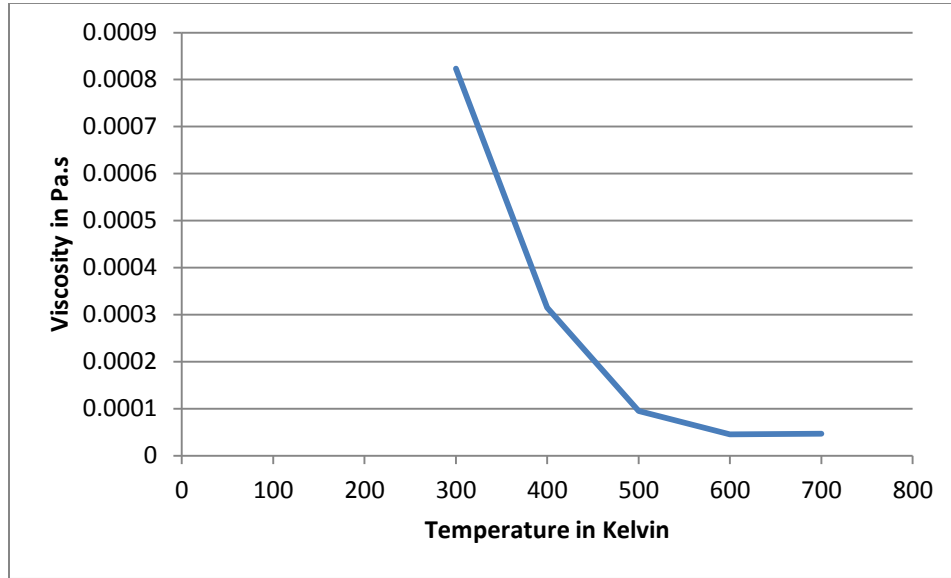
ds=[d];
ds=ds(:);
```

```
function ds=lignin_ode(t,s,teta);
A=s(1); %lignin
B=s(2); %Toc
C=s(3); %gas
D=s(4); %char
T=573;
dadt=-teta(1)*A-teta(2)*A-teta(3)*A;
dbdt=teta(1)*A;
dcdt=teta(2)*A;
dddt=teta(3)*A;

% d=[-k1*A
%     k1*A-k2*B
%     k2*B];
ds=[dadt dbdt dcdt dddt];
ds=ds(:);
```

```
function ds=hemi_ode(t,s);
H=s(1);
O=s(2);
% T=573;
% R=8.314;
k=6.35e-1;
% k=0.017;
%
da=-k*H;
db=k*H;
ds=[da db];
ds=ds(:);
```

## Appendix F: Viscosity and Conductivity inside the reactor; calculated by ANSYS fluent



**Appendix G: Modeling of Particles at different sizes (50,150,600 and 1100)**

**mm.**

